coatings

MDPI

Review

A Review of Crack Sealing Technologies for Asphalt Pavement: Materials, Failure Mechanisms, and Detection Methods

Weihao Min [1], Peng Lu [1], Song Liu [1,2,*] and Hongchang Wang [1,2]

[1] College of Civil Engineering, Nanjing Forestry University, Nanjing 210037, China; minwh@njfu.edu.cn (W.M.); simple@njfu.edu.cn (P.L.); seuwhc@126.com (H.W.)
[2] Jiangsu Highway Intelligent Detection and Low-Carbon Maintenance Engineering Research Center, Nanjing 210037, China
* Correspondence: ls2020@njfu.edu.cn; Tel.: +86-025-85427115

Abstract

Asphalt pavement cracking represents a prevalent form of deterioration that significantly compromises road performance and safety under the combined effects of environmental factors and traffic loading. Crack sealing has emerged as a widely adopted and cost-effective preventive maintenance strategy that restores the pavement's structural integrity and extends service life. This paper presents a systematic review of the development of crack sealing technology, conducts a comparative analysis of conventional sealing materials (including emulsified asphalt, hot-applied asphalt, polymer-modified asphalt, and rubber-modified asphalt), and examines the existing performance evaluation methodologies. Critical failure mechanisms are thoroughly investigated, including interfacial bond failure resulting from construction defects, material aging and degradation, hydrodynamic scouring effects, and thermal cycling impacts. Additionally, this review examines advanced sensing methodologies for detecting premature sealant failure, encompassing both non-destructive testing techniques and active sensing technologies utilizing intelligent crack sealing materials with embedded monitoring capabilities. Based on current research gaps, this paper identifies future research directions to guide the development of intelligent and sustainable asphalt pavement crack repair technologies. The proposed research framework provides valuable insights for researchers and practitioners seeking to improve the long-term effectiveness of pavement maintenance strategies.

Keywords: asphalt pavement; crack sealing; sealing material; failure mechanisms; active sensing

check for updates

Academic Editor: Valeria Vignali

Received: 30 June 2025
Revised: 15 July 2025
Accepted: 16 July 2025
Published: 17 July 2025

Citation: Min, W.; Lu, P.; Liu, S.; Wang, H. A Review of Crack Sealing Technologies for Asphalt Pavement: Materials, Failure Mechanisms, and Detection Methods. *Coatings* **2025**, *15*, 836. https://doi.org/10.3390/coatings15070836

Copyright: © 2025 by the authors. Licensee MDPI, Basel, Switzerland. This article is an open access article distributed under the terms and conditions of the Creative Commons Attribution (CC BY) license (https://creativecommons.org/licenses/by/4.0/).

1. Introduction

Asphalt pavement represents the predominant pavement structure found in modern transportation infrastructure, serving as the backbone of global road networks. Under prolonged exposure to complex environmental factors and repetitive traffic loading, pavement distress has emerged as a critical factor significantly affecting the structural performance and service quality of asphalt pavements. Rutting typically precedes cracking in asphalt pavements—a fundamental pattern that is rooted in rut formation, this being the cumulative plastic deformation of mixtures under high-temperature and heavy-load conditions, whereas cracking results from stresses exceeding material strength. Rutting constitutes not only initial distress but is also a significant precursor to subsequent cracking. Through mechanisms including stress redistribution, accelerated material deterioration, water ponding,

and weakened interlayer bonding, rutting establishes the conditions for diverse cracking modes. However, among various early-stage distress signs in asphalt pavements, cracking is undoubtedly the most prevalent and critical form, requiring prioritized attention [1–4]. Without timely and effective intervention, cracks facilitate water infiltration into the underlying pavement structural layers, thereby accelerating deterioration processes and ultimately progressing to more severe distress, including potholes and alligator cracking, which pose substantial risks to traffic safety and operational efficiency [5].

Among the various crack repair strategies available, specific measures—such as microsurfacing, sealing, mill-and-replace, or crack-sealing tape—are implemented based on crack severity. Crack sealing technology has gained widespread acceptance due to its straightforward construction procedures and cost-effectiveness, establishing itself as an economically viable preventive maintenance approach [6]. The process of filling cracks with specialized sealing materials serves multiple critical functions: restoring pavement structural integrity and surface continuity, blocking the moisture penetration pathways into deeper pavement layers, preventing the subgrade bearing capacity reduction associated with elevated moisture content, and significantly retarding further crack propagation. These combined effects contribute to substantial extensions in pavement service life. The long-term effectiveness of crack sealing interventions depends critically on the stability and durability characteristics of the sealing materials employed [7–11]. High-performance crack sealing materials must demonstrate sustained adhesive properties and elastic behavior under variable temperature conditions and dynamic loading scenarios in order to prevent secondary cracking and interfacial debonding phenomena following repair implementation.

Material properties fundamentally govern crack repair effectiveness and long-term performance. Optimal crack sealing materials should exhibit a comprehensive suite of performance characteristics, including superior flowability for adequate crack penetration, strong adhesion for robust interfacial bonding, sufficient flexibility to accommodate thermal and traffic-induced deformations, exceptional durability for extended service life, and dimensional stability under varying environmental conditions. These properties collectively ensure that sealing materials can effectively penetrate crack geometries, establish high-strength bonds with crack surfaces, accommodate pavement deformation cycles without failure, and maintain crack resistance performance throughout their design life.

Recent advances in materials science have facilitated substantial performance enhancements in crack sealing materials through the strategic incorporation of novel additives, particularly nanomaterials, resulting in markedly improved adhesive characteristics and durability performance [12–15]. The emergence of intelligent crack sealing materials incorporating self-sensing and self-healing functionalities has introduced autonomous damage monitoring capabilities, providing innovative technological support for the evolution of pavement maintenance toward intelligent and precision-oriented paradigms [16,17]. Complementary developments in non-destructive testing technologies have enhanced crack repair quality assessment capabilities [18–23], enabling the rapid and accurate evaluation of sealing material placement density and in-service condition assessment. The synergistic application of these technological advances contributes to the enhanced durability of asphalt pavement crack sealing systems, enables the dynamic monitoring and quantitative evaluation of damage progression, and provides robust theoretical foundations for ensuring the long-term stability of crack-repaired asphalt pavements.

This comprehensive review systematically examines the evolutionary development of asphalt pavement crack sealing technology in cold and seasonally frozen regions of China, provides a comparative analysis of the performance characteristics, advantages, limitations, and application domains of various sealing materials, and critically evaluates the existing performance assessment methodologies. The review integrates consideration of the key

influencing factors, including construction processes, material aging mechanisms, traffic loading effects, and thermal cycling impacts, to thoroughly analyze secondary cracking behavior and failure mechanisms in sealed crack systems. Furthermore, this paper explores the emerging active sensing technologies for crack damage behavior assessment, utilizing intelligent sealing materials, and investigates the development trajectories for intelligent operation and maintenance frameworks in asphalt pavement crack management. This review aims to provide comprehensive theoretical guidance and technical insights to support continued advancements in asphalt pavement crack repair technology, facilitating the development of crack sealing materials and condition monitoring systems toward increasingly intelligent and sustainable operational paradigms.

2. Materials and Performance Evaluation for Asphalt Pavement Crack Sealing

2.1. Development of Asphalt Pavement Cracks

Under the combined effects of traffic loads, temperature fluctuations, and moisture infiltration, asphalt pavements inevitably develop various signs of distress with extended service life. Cracking represents one of the most prevalent and critical defects in asphalt pavements, as shown in Figure 1 [24,25]. During the initial stage of crack formation, the pavement maintains adequate road performance. However, as the cracks progressively expand and deepen over time without timely intervention, significant reductions in both the stiffness and strength of the asphalt surface layer will occur.

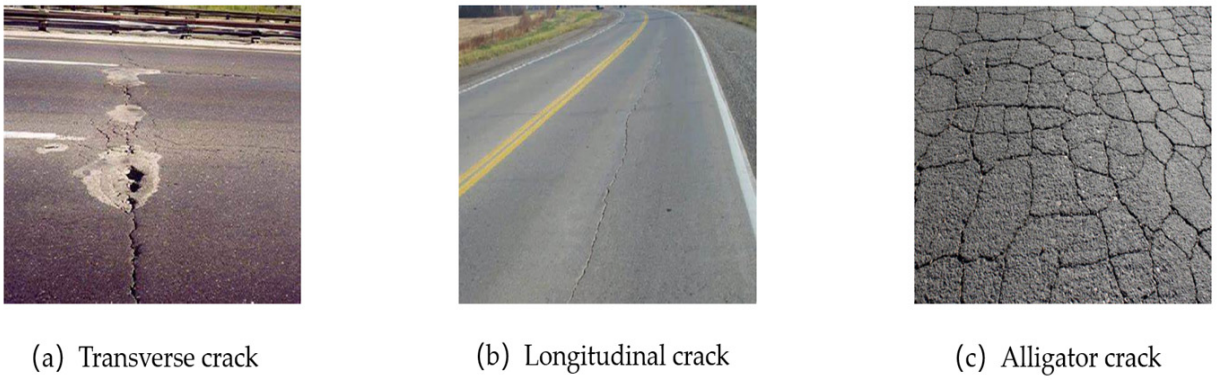


Figure 1. Cracking of asphalt pavement.

During crack propagation, crack morphology plays a critical role, primarily manifesting as transverse and longitudinal cracks. Transverse cracks mainly result from reflective cracking: under combined traffic loading and thermal stress, thermal shrinkage and desiccation cracks develop in semi-rigid base layers and propagate upward into the asphalt's surface layers. Conversely, longitudinal cracks originate within asphalt layers due to material aging and the fatigue damage induced by repetitive environmental exposure and loading effects.

Furthermore, regional crack investigations provide proactive guidance for maintenance strategies. Wang et al. [26] examined 202 cross-sections across 11 expressways in Jiangsu Province (2015–2018), collecting 1003 core samples for crack morphology analysis. The results revealed that over 80% of cracked samples exhibited simultaneous failure in both the asphalt surface and base layers, while only 5.9% displayed cracking behavior confined to the asphalt surface layer. Consequently, the service performance and lifespan of asphalt pavements in preventive maintenance scenarios are largely determined by the appropriateness and effectiveness of the sealing techniques applied to different crack types.

For asphalt pavement cracks, primary considerations include crack width, the selection of sealing methods/materials, and the restoration of road performance post-repair. This

study focuses on sealing treatments for early-stage cracks (micro-cracks with widths of < 2 mm), examining both the flow characteristics of the sealing materials and their interfacial bonding with the existing pavement, while evaluating whether original road performance can be restored after rehabilitation. Crack severity classifications are detailed in Table 1.

Table 1. Physical technical indicators of MCR.

Crack Type	Severity Level	Pavement Manifestation	Crack Width (mm)
Alligator Cracking	Slight	Fine shallow patterns, non-networked, no spalling	≤2
	Moderate	Deepened cracks, localized networking with debris	2~5
	Severe	Dense networked cracking, fragmentation settlement, and base layer exposure	≥5
Longitudinal and transverse crack	Slight	Minor raveling adjacent to the crack/no loose material, few secondary cracks	≤3
	Severe	Significant raveling adjacent to the crack, numerous secondary cracks	≥3

2.2. Crack Repair Methods

Current pavement maintenance primarily employs two crack repair methods: the tape-sealing technique and crack sealant-sealing treatment.

The tape-sealing technique mechanically compresses sealing strips to close up cracks, functioning as a "band-aid" solution for pavement fractures. This method eliminates the need for crack routing—only surface cleaning is required prior to application, significantly enhancing operational efficiency while preventing the secondary distress induced by routing operations. Field implementation and monitoring by Li et al. [27] demonstrated the temporary absence of adhesive failure or cracking in most installed tapes. However, this method only provides effective sealing for shallow cracks. Prolonged exposure to traffic causes tape dislodgment, where the adhesive bonding transfers to vehicle tires, resulting in material loss and low retention rates of tape repairs [28].

Crack sealant-based sealing treatments, as an emerging technology under current promotion, are increasingly applied for repairing micro-cracks in asphalt pavements. In contemporary road maintenance engineering, traditional materials such as thermal asphalt and emulsified asphalt remain primary choices for crack sealing. However, these conventional materials exhibit inherent limitations. Thermal asphalt demonstrates significant technical constraints, as it merely seals the crack surfaces with poor wall adhesion and shows high susceptibility to re-cracking under low-temperature conditions. In contrast, while emulsified asphalt outperforms in terms of permeability, its post-curing strength and bonding performance are inferior to hot-applied materials, coupled with inadequate durability.

To address the material limitations and standardize construction protocols, the Technical Specifications for Highway Asphalt Pavement Maintenance (JTG 5142-2019) [29] stipulate routing decisions based on crack width, with the following criteria:

(1) Routing is recommended when the measured crack width is ≥3 mm.
(2) For cracks exhibiting a high probability of horizontal movement under thermal variation, field assessment mandates routing prior to sealant application.

The criteria for routing-free treatment are specified as follows:

(1) When the crack width measures < 3 mm and demonstrates self-healing capability under thermal cycling, routing-free sealing shall be applied.
(2) Cracks exhibiting negligible horizontal displacement may undergo routing-free treatment following a techno-economic assessment.

(3) For cracks 1–3 mm wide, the crack wall conditions dictate the methodology: intact walls without spalling/raveling permit direct sealing; walls with loosening surfaces, oil contamination, or irremovable debris require routed sealing [30].

Comparative analysis reveals that while the tape-sealing technique offers operational efficiency advantages for the rapid treatment of shallow surface cracks, its durability limitations and restricted applicability constrain its long-term performance. Conversely, crack sealant-based sealing technology achieves the comprehensive filling of crack depth and width through material innovation, standardized protocols, and superior flow characteristics. Coupled with exceptional bonding performance, this method proves unbeatable for mitigating moisture damage and extending pavement service life.

Consequently, sealant-based sealing constitutes not merely the current mainstream repair technique but is also the cornerstone of systematic crack preservation. Its specification-compliant implementation significantly enhances roadway service performance.

2.3. Sealing Material Selection

Sealing materials used for sealant-based sealing treatment are primarily categorized as conventional, ambient-temperature, and hot-applied types [31].

Designed for surface cracks of $\leq$3 mm wide, these materials must exhibit sufficient post-heating flowability to ensure thorough penetration, preventing viscosity-induced sealing failures.

2.3.1. Conventional Sealing Materials

Conventional crack sealants, such as emulsified asphalt and hot-applied asphalt [32,33], exhibit favorable fluidity and bonding performance at elevated temperatures. Characterized by lower costs and well-established construction techniques, they are typically employed as the primary choice for repairing microcracks. In contrast, advanced crack sealants are formulated from polymer-, rubber-, polyurethane-, or resin-modified asphalt [34–37]. These modification materials enhance fluidity and interfacial bond strength through targeted additive incorporation.

Zhang et al. [32] demonstrated that hot-applied asphalt surpasses traditional asphalt tape as a joint material in mechanical performance. It effectively enhances the bonding strength at joints and reduces the cracking risks caused by vehicular loading and structural deformation. Through a comparative analysis of conventional, high-viscosity modified, and resin-modified emulsified asphalt, Shao et al. [33] determined that high-viscosity modified emulsified asphalt applied at 0.6 kg/m^2 on a 30° inclined surface achieved the maximum interface joint fatigue life and bond strength.

2.3.2. Ambient-Temperature Sealing Materials

Room-temperature crack sealants primarily comprise three material types: polyurethane, polysulfide, and resin.

Liu et al. [34] developed a thermoplastic polyurethane-modified asphalt (TP-MPUA) and conducted peel tests on specimens containing 0 wt.% and 6 wt.% of modifier. These tests simulated the effects of external conditions—dust, water, and low temperatures—on adhesion performance. The results demonstrated that TP-MPUA exhibited superior interfacial bonding and low-temperature deformation resistance under dusty and low-temperature conditions. However, exposure to water resulted in greater material loss compared to asphalt alone.

Polysulfide sealants exhibit advantages such as uniform curing performance and good climatic adaptability, yet their bonding performance remains relatively moderate. Consequently, these sealants are frequently modified through various physical and chemical

methods. Teng et al. [35] enhanced polysulfide sealants using graphene oxide (GO) as a modifier. Their findings revealed that the maximum strength was achieved at a GO dosage of 0.2 phr. Compared to unmodified polysulfide sealant, this modified version demonstrated a 24.7% increase in tensile strength and a 21.7% improvement in bond strength.

Chang et al. [36] evaluated the performance characteristics of epoxy resin/powder curing agent repair materials using four key metrics: permeability, bonding performance, low-temperature crack resistance, and water stability. Separately, Tan et al. [37] measured the complex shear modulus (CSM) of asphalt sealants containing epoxy resin microcapsules using dynamic shear rheometry (DSR). As depicted in Figures 2 and 3, the maximum CSM value was achieved at a 3% microcapsule dosage, indicating superior self-healing capability in the sealant at this concentration. The repair index (PN) indicates that the fatigue life of microcapsule-containing material after a 1-hour repair is lower than that of the unmodified base material. As evidenced in Figure 3, PN values remain below the original level. This occurs because the epoxy resin requires 48 h of room-temperature curing to achieve optimal performance, while the 1-hour repair duration is insufficient for complete resin curing.

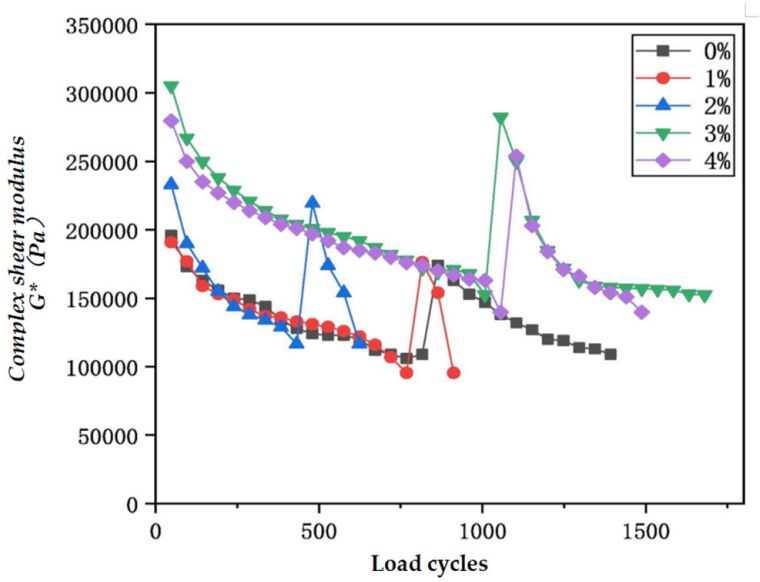


Figure 2. Complex shear modulus of ACSM [37].

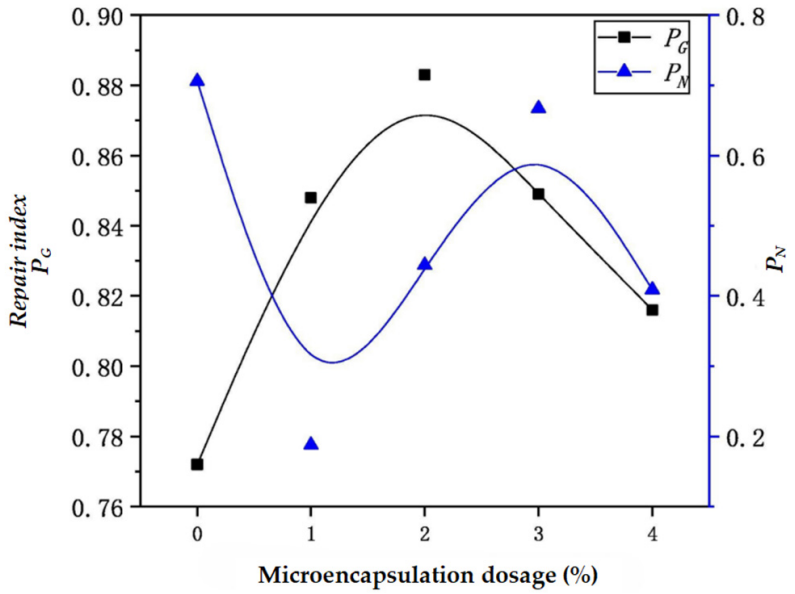


Figure 3. Repair index of ACSM [37].

Fu et al. [38] conducted a comparative analysis of five sealing materials—polysulfide-urethane, silicone, polysulfide, polyurethane, and modified polyurethane—evaluating their comprehensive properties and bond strength. Their findings highlight that polysulfide-urethane sealants not only inherit the exceptional barrier performance of polysulfide sealants against water and other media, but also effectively address key limitations: specifically, they mitigate the inadequate UV resistance inherent in polysulfide sealants while concurrently resolving issues prevalent in polyurethane sealants, such as bubble formation, cracking susceptibility, poor long-term resistance to humid-heat environmental degradation, and inferior aging performance.

2.3.3. Heat-Applied Sealing Materials

Hot-poured crack sealants typically refer to rubber-modified asphalt sealants, which incorporate ground rubber powder particles. The size of these particles influences sealant properties. Larger particles increase softening point, viscosity, and elastic recovery. They also significantly enhance the asphalt's fatigue resistance. Conversely, smaller particles disperse more effectively during mixing, improving thermal storage stability [39].

Yan et al. [40] found that asphalt crack sealants modified with CR and PU exhibited excellent sealing performance, durability, and water resistance. Using Grey Relational Analysis (GRA), Gong et al. [41] assessed the influence of SBS and CR on the high-temperature performance of modified asphalt-based sealants. Their results revealed that SBS content exhibited a stronger correlation with the sealant's high-temperature performance than CR content. Liu et al. [42] further investigated SBS/CR composite-modified asphalt crack sealants. By incorporating highly polar ethylene-vinyl acetate (EVA) copolymer to broaden the polarity gradient, they enhanced the interactions between the different modifiers and between the modifiers and the asphalt. This optimization improved the sealant's rheological properties and its viscoelastic behavior.

In summary, selecting appropriate sealing materials and repair methods based on environmental conditions and crack dimensions is crucial. All three sealant types exhibit good fluidity upon heating. However, conventional sealants demonstrate relatively poor durability and higher environmental sensitivity. Ambient-temperature sealants require performance-enhancing modifications tailored to specific environments. The performance of hot-poured sealants can be optimized by controlling rubber powder particle size: larger particles improve fatigue resistance, while smaller particles enhance high-temperature stability. Future sealing materials should feature enhanced rheological properties, bond strength, and environmental adaptability through composite material systems. Coupled with optimized preparation processes to reduce the curing time, these improvements will extend the service life of sealed-crack asphalt.

2.4. Performance Assessment of Sealing Material

Significant research has been conducted, both domestically and internationally, to effectively evaluate the performance of sealing materials. As the primary international evaluation system for sealing materials, American Society for Testing and Materials D6690-12 (ASTM D6690-12) categorizes them into four distinct types, based on their regional temperature characteristics [43]. This classification specifies the critical performance requirements for each type, including penetration, softening point, low-temperature tensile properties (both when dry and after water immersion), elastic recovery, and elastic recovery after aging. Standards in Europe and other countries have largely been adapted from the ASTM framework [44]. Furthermore, Soliman et al. [3] utilized bending beam rheometer (BBR) testing to establish the evaluation metrics for crack sealants, specifically load decay tension at −30 °C and complex shear modulus (G*) at 5 °C. Liu et al. [45] evaluated the

low-temperature crack resistance of crack sealants using low-temperature ductility test values. Their results indicated that at the same test temperature of 5 °C, the measured ductility values of the materials were reduced to half of their initial values. Li et al. [46] conducted softening-point tests using the ring-and-ball method. Their findings demonstrated that the softening-point value reflects the high-temperature stability of the sealant materials. Yan et al. [47] assessed the bonding condition between sealing materials and crack walls via pull-off tests. They found that the pull-off strength of the sealing material decreased significantly with increasing temperature.

Due to the complexity of field construction environments, current performance standards cannot comprehensively evaluate repair materials. Consequently, researchers have developed multiple testing methods to better assess the bonding performance of crack sealants [48]. Sun et al. [49] validated the feasibility of surface energy theory for bonding assessment through multi-method verification, including the sessile drop method, a modified boiling test, and digital image processing (DIP).

The inconsistent units in evaluation metrics impede a comprehensive assessment of crack sealant service performance. To address this issue, researchers have developed novel evaluation frameworks. Wang et al. [50] established a performance evaluation system for crack sealants in seasonally frozen asphalt pavements using an entropy weight-TOPSIS methodology. Normalization processing eliminates dimensional differences among indicators, enabling the direct comparison of physical parameters such as viscosity (Pa·s), penetration (0.1 mm), and tensile stress (MPa). This approach resolves multi-dimensional data integration challenges while facilitating the simultaneous assessment of both short- and long-term bonding performance. Li et al. [51] proposed an integrated evaluation method: assigning appropriate scores and weights to each performance indicator to calculate comprehensive performance values, ultimately classifying and ranking crack sealants based on their total performance scores.

In summary, as a primary solution for pavement crack rehabilitation, the performance evaluation system of crack sealants has been progressively refined through extensive research. However, two critical technical challenges persist in engineering practice: firstly, inadequate bonding effectiveness during construction due to insufficient flowability or suboptimal application techniques; secondly, vulnerability to secondary cracking during service life under multi-factor influences, including thermal cycling and water ingress. To overcome these limitations, future research should prioritize developing failure mechanism models based on multi-factor coupling effects. This entails quantitative analysis of damage evolution under environmental-load synergistic actions. Concurrently, establishing a whole-lifecycle evaluation system is essential, incorporating real-time pavement monitoring with feedback through digital platforms for timely crack intervention. Ultimately, this integrated approach will mitigate secondary cracking risks and prolong the pavement's service life.

3. Early-Stage Failure Mechanisms in Sealed-Crack

3.1. Interfacial Bond Failure Induced by Construction Defects

The crack sealing procedure typically comprises eight sequential steps: traffic closure, preparation, routing, cleaning, drying, sealing, aggregate spreading for curing, and quality inspection, as shown in Figure 4. The service life of sealed-crack repairs is directly determined by the extent of debris removal and the filling fullness index during crack sealing. Furthermore, the precise thermal regulation of the sealing material during application ensures a dense filling through optimal material fluidity.

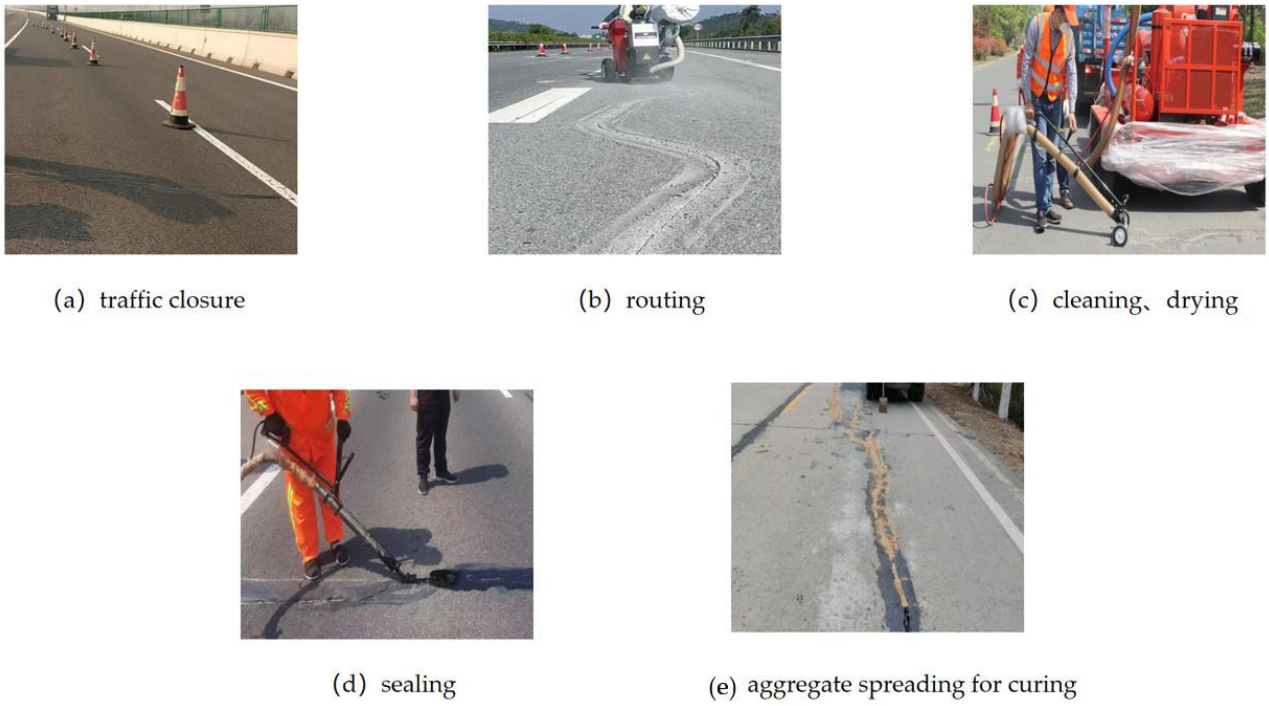


Figure 4. Flowchart of the crack sealing process.

(1) Inadequate crack cleaning

Thorough crack cleaning and drying are essential preparatory procedures. Unclean or moist crack walls reduce their adhesion to sealants, resulting in interfacial bonding failure. Performance comparisons of various sealing materials under moist versus dry conditions [51] demonstrate that dry-crack sealing achieves 2–4 times longer service life than when sealant is applied to moist cracks.

(2) Crack wall heating temperature

Prior to sealing, sealants are typically heated to approximately 180 °C. Insufficient heating of the crack walls compromises bonding efficacy, due to thermal differentials, whereas excessive heating accelerates asphalt aging, manifesting as aggregate stripping, wall disintegration, or binder degradation. Therefore, crack wall heating must be coordinated with sealant heating within an optimal thermal window.

Lin et al. [52] conducted six simulation experiments with controlled heating and sealing temperatures to determine the optimal crack wall temperatures. Lai et al. [53] performed tensile testing on six specimen groups at −30 °C. Both studies established 140 °C as the optimal crack wall heating temperature, with specimens exhibiting cracking at specific tensile deformation thresholds. Reheating is recommended when crack wall temperatures fall below the 70 °C critical threshold. Furthermore, adaptive temperature reduction is required for pavements containing emulsified or modified asphalt binders.

(3) Sealing Material Application Temperature

The selection of application temperature critically governs sealing material workability and bonding integrity. Suboptimal temperatures reduce fluidity, impeding crack penetration and inhibiting infiltration into asphalt micro-pores. This compromises the wetting action at sealing material–wall interfaces, diminishing sealing efficacy. Conversely, excessive temperatures enhance flow properties but accelerate thermal degradation, with hyperfluidity causing viscosity loss and durability reduction beyond the permissible thresholds for construction specifications.

Following the Test Methods for Asphalt and Asphalt Mixtures in Highway Engineering (JTG E20-2011) [54], the viscosity of sealing materials was measured using a Brookfield viscometer. Testing temperatures were typically set at 150 °C, 160 °C, 170 °C, 180 °C, and 190 °C. Appropriate spindle models were selected according to sealing material viscosity, with measurements conducted at fixed rotational speeds (e.g., 15 r/min) under varying temperatures. Torque readings were maintained within the 10%–98% valid measurement range throughout testing. Finally, regression analysis established the correlation curves between viscosity values and the corresponding torque measurements at specified rotational speeds.

Feng et al. [55] performed regression analysis on Brookfield rotational viscosity test results to establish the viscosity–temperature curve of the crack sealant. This analysis determined the optimal construction temperature to be 182 °C. Further verification confirmed that the Brookfield rotational viscosity at 190 °C was 2.438 Pa·s, which complies with the technical requirement of 1–3 Pa·s for crack sealants proposed by Li et al. [56].

(4) Injection volume of the sealing material

Precise control of the injection volume is critical to ensuring effective sealing and long-term durability. The influence of injection volume on repair performance is detailed in Table 2.

Table 2. Hazards of inadequate or excessive injection volume.

Problem Type	Specific Manifestations	Consequences
Inadequate Injection	Incomplete filling, presence of voids	Water infiltration exacerbation, bond failure, crack propagation.
Excessive Injection	Material overflow, surface bulging	Unnecessary material waste, extrusion deformation under traffic loading, compromised skid resistance.

In summary, to achieve optimal bonding in sealed cracks:

- The preparation phase involves precisely measuring crack width and depth and thoroughly removing debris from the crack periphery.
- In the construction phase, nozzles compatible with the crack width are selected, and the heating temperature of the sealing material is strictly controlled.
- In process monitoring, operators should continuously observe the filling status and surface bulging, dynamically adjusting the injection equipment speed to maintain consistent operation.

3.2. Aging Behavior of Sealants

Although both thermal–oxidative aging and UV aging accelerate asphalt decomposition, they represent fundamentally distinct degradation processes [57]. Regarding thermal–oxidative aging, the elevated temperature during crack sealing material application causes the volatilization of light components. These components act as a "solvent," reducing the overall viscosity. However, their depletion increases the relative proportion of asphaltenes, resulting in increased binder hardness, reduced fluidity, and impaired high-temperature stability.

The degree of asphalt aging was evaluated using penetration, softening point, ductility, and rheological properties as assessment indicators. Research has demonstrated that asphalt becomes harder and more brittle after undergoing varying degrees of thermal–oxidative aging [58,59]. Xie et al. [60] analyzed the micromorphology of asphalt before and after aging, as shown in Figure 5. From left to right, these are original, TFOT aging, and PAV aging. Their analysis revealed that with increasing aging severity, in both asphalt types, the

fewer the bee-shaped structures, the larger the area of a single bee-shaped structure, and the less bright the white convex marks will be. Camargo et al. [61] employed NAAT and OAAT to assess the effects of thermal aging and oxidative aging on asphalt pavement binders. Their results demonstrated that the mass loss due to oxidative aging of the material was greater than the mass loss resulting from volatilization during thermal aging.

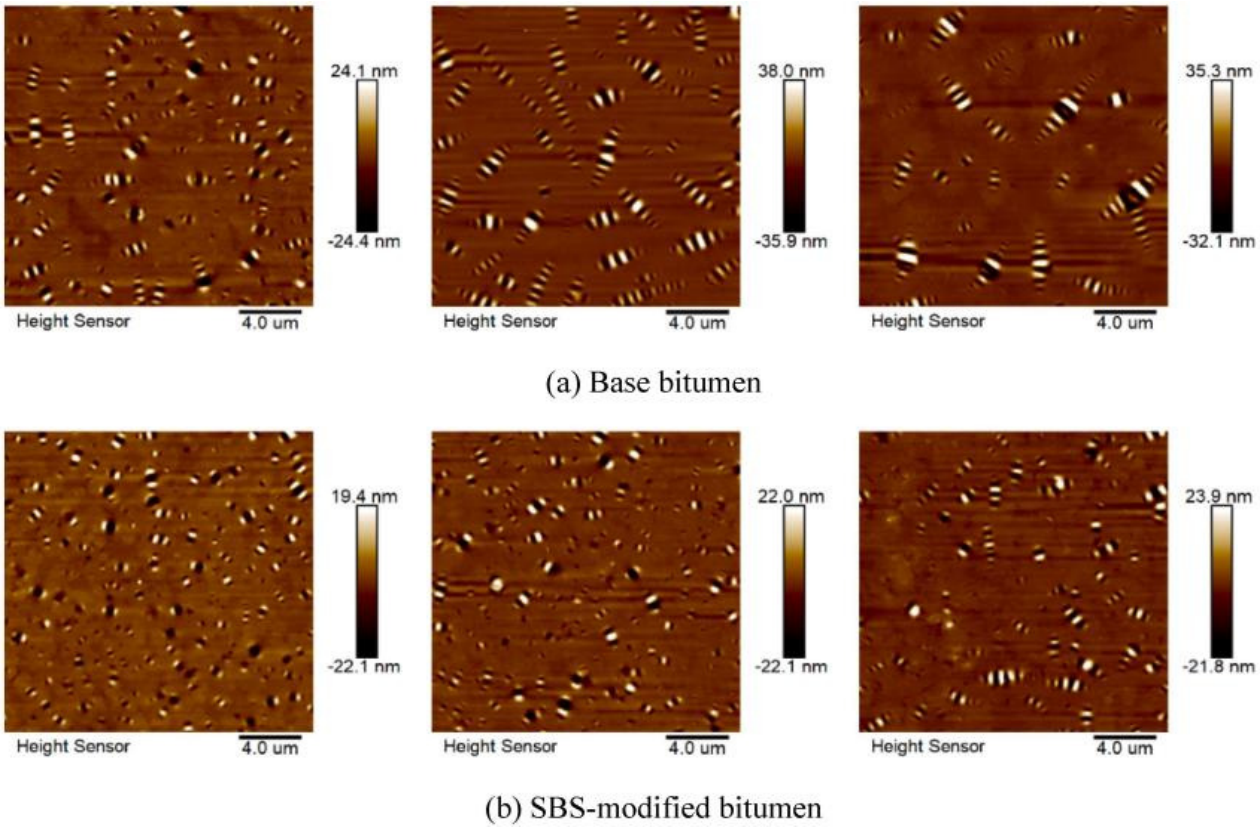


Figure 5. Micromorphology of base bitumen and SBS-modified bitumen under different aging degrees [60].

In UV aging, following sealed crack repair, portions of the sealing material remain exposed on the pavement surface. Prolonged exposure to ultraviolet (UV) radiation causes the surface and bulk properties of the sealing material to undergo gradual aging and deterioration. Hung et al. [62,63] investigated the surface characteristics and chemical composition of asphalt binders subjected to UV radiation. Their research revealed a notable decrease in aromatic compounds and olefins within the asphalt fractions after UV aging compared to their unaged state.

UV-A radiation (wavelength 300–420 nm) constitutes the primary spectral band responsible for the aging of crack sealants [64]. Li et al. [65] conducted aging simulation experiments using five distinct UV radiation sources. These sources shared a fixed half-wave band and identical irradiation intensity but varied in their dominant wavelengths. Their experimental results demonstrated that UV-360 radiation induced the most severe degradation in the asphalt binder. While all UV radiation contributes to asphalt aging and degradation, this does not imply that shorter-wavelength UV radiation (possessing higher photon energy) inevitably causes the most severe asphalt aging.

Given the disparities between natural environments and laboratory simulations, Yang et al. [66] focused their research on investigating the performance changes of crack sealants exposed to natural solar radiation for eight months. This approach aimed to establish a theoretical relationship between indoor UV aging and outdoor natural radiation aging. To

further investigate the UV aging mechanism of crack sealants, Yang et al. [67] subjected two types of sealants to UV aging for 0–385 h using a UV-A 365 nm lamp with a fixed intensity and temperature. Analysis of the Fourier transform infrared (FTIR) spectroscopy results, as illustrated in Figure 6, revealed that UV radiation induced the volatilization of light components within the crack sealants and increased the molecular weight of the polymer modifiers. These findings imply that under UV exposure, the asphalt-based components of the crack sealant undergo inevitable aging, while the polymer particles experience degradation.

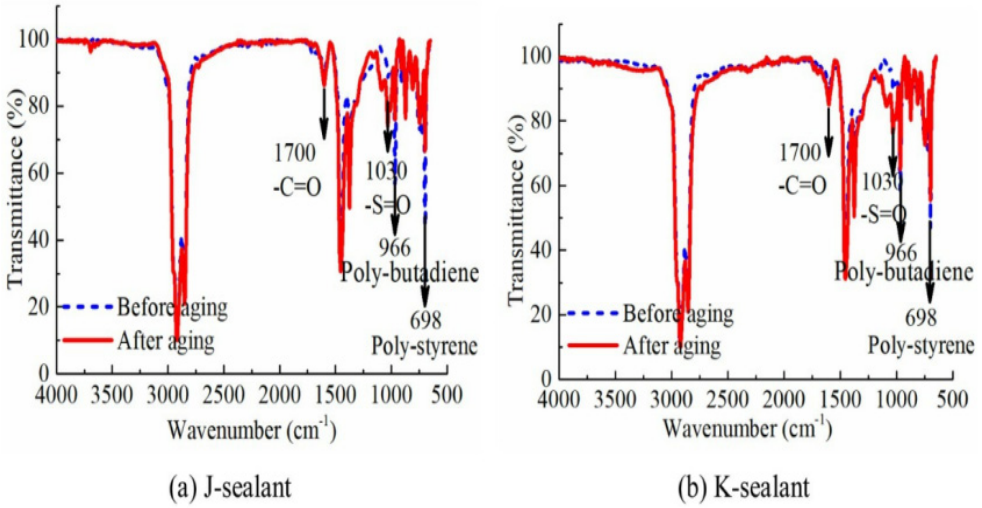


Figure 6. Infrared spectra of sealants before and after natural aging [67].

3.3. Hydrodynamic Scouring Effects

During rainfall, a thin water film typically forms on pavement surfaces. Under vehicle loading—particularly in high-speed traffic—this film instantaneously generates significant hydrodynamic pressure [68].

Hydrodynamic pressure generates dynamic impact forces through water flow within the cracks, inducing shear stress concentration at the sealing material–crack wall interface. This triggers a physical separation between the aggregates and asphalt binder films, consequently degrading interfacial bonding performance. The magnitude of hydrodynamic pressure is governed by water film thickness, vehicle speed, porosity, and other factors. From a vehicular perspective, axle load and travel speed constitute the primary factors influencing hydrodynamic pressure in asphalt pavements. Gao et al. [69] demonstrated that under saturated pavement conditions, the hydrodynamic pressure induced by low-speed heavy loads causes significant pavement damage. Complementary research [70] further confirms the substantial damaging effect of hydrodynamic pressure under heavy loading conditions. Experimental data from Wang et al. [71] indicate that pore water pressure at 20 km/h is 9.54 times that at 80 km/h. From a hydrodynamic perspective, water film thickness constitutes the primary influencing factor. Dong et al. [72] demonstrated that hydrodynamic pressure increases gradually with vehicle speed when the water film thickness is below the tire tread pattern depth, whereas when it exceeds this critical depth, hydrodynamic pressure exhibits a near-linear proportionality to vehicle speed.

Given the challenges in direct measurement of hydrodynamic pressure, numerical simulation provides an effective analytical alternative. Employing COMSOL5.4-based finite element simulation, Zhang et al. [73] demonstrated that surface layers in dense-graded asphalt pavements experience more severe hydrodynamic damage than intermediate/base layers. Variations in the permeability coefficients of upper-layer materials significantly influence hydrodynamic pressure. As illustrated in Figure 7, hydrodynamic pressure in

the surface/upper layers increases inversely with the permeability coefficient, whereas sub-base regions exhibit negligible variation [70].

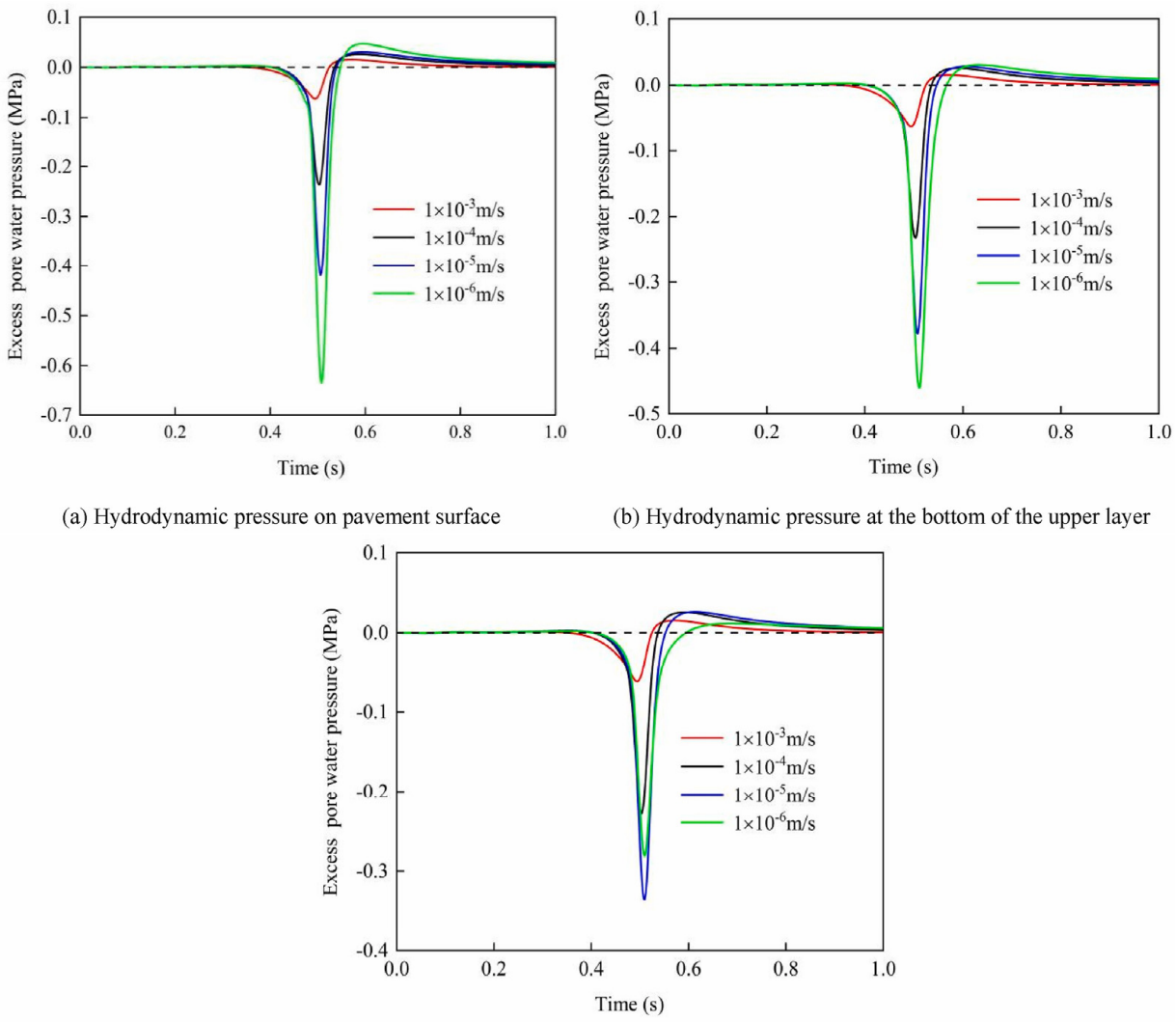


Figure 7. Hydrodynamic pressure under different permeability coefficients [68].

3.4. Temperature Effects

In most seasonally frozen regions, significant temperature differences exist between winter and summer. An investigation by Lin et al. [52] on crack development along five expressways in Heilongjiang Province revealed seasonal crack width variations exceeding 10 mm, with maximum differentials reaching 22 mm. Such thermal variations inevitably cause severe damage to sealed-crack repairs. Through the year-long monitoring of asphalt pavement crack widths, Feng et al. [74] determined the optimal sealing temperature to be approximately 10.2 °C. They further proposed April–May and September–October as the optimal periods for crack sealing operations.

The random cracking index (RCI) metric accounts for all random cracks, including transverse, longitudinal, block, and reflective cracks [75], as expressed in Equation (1). Mousa et al. [76] investigated cracks in asphalt concrete overlays under hot and humid climatic conditions in Louisiana. Their findings identified an RCI range of 81–89 as the optimal intervention timing for crack repair.

$$\mathrm{RCI} = \min\{100 \times \max(0.100 - \mathrm{DP_L} - \mathrm{DP_M} - \mathrm{DP_H})\} \quad (1)$$

DP denotes the random deduction points caused by cracking, while L, M, and H represent the low, medium, and high severity levels of cracks, respectively.

4. Advanced Sensing Methodologies for Premature Sealed-Crack Repair Failure

Following the repair of cracked pavement surfaces, dynamic monitoring of sealing performance, material bond strength, and edge bonding conditions at the sealed-crack repair is required. Particularly in road sections exhibiting significant seasonal temperature differences, high annual precipitation, daily traffic exceeding 5000 standard axle passes, interfacial stress concentration due to thermal expansion and contraction, moisture damage at interfaces caused by repeated rainwater infiltration, and material fatigue deterioration from sustained heavy-duty vehicle vibrations frequently lead to premature interfacial bond failure, material loss, and water seepage within the anticipated 3–5 year service life.

Core drilling and visual inspection serve as early-warning methods for assessing pavement service performance. These labor-intensive and time-consuming approaches fail to meet current efficiency demands for pavement evaluation. Moreover, core drilling adversely affects pavement structures, compromising the integrity of structural layers. Furthermore, nuclear density gauges partially fulfill nondestructive testing requirements. They enable a compaction quality assessment of sealed-crack repairs and reflect grout material density to some extent, yet they pose radiation hazards and require specialized operator training.

Collectively, traditional detection methods exhibit three primary limitations:

① Structural impact on pavements;

② Slow inspection speed;

③ Significant manpower and time requirements.

Consequently, high-efficiency and high-precision detection techniques are required to address current road crack identification needs.

Therefore, periodic inspection mechanisms should be established. This paper presents passive detection and active sensing approaches, detailing the application of three NDT technologies for asphalt pavement cracks. Additionally, the feasibility of piezoresistive materials for active pavement condition sensing is discussed in the context of intelligent transportation trends.

4.1. Passive Sensing Technologies

4.1.1. Ground-Penetrating Radar (GPR)

Road subsurface damage (RSD) refers to structural defects occurring beneath pavement surfaces (in base courses, subgrades, and subsoils) [77]. The most prevalent RSD manifestations include voids, cracks, and differential material settlement, which frequently lead to severe incidents such as road collapse. Ground-penetrating radar (GPR) has emerged in recent years as an effective subsurface detection method. Its operational principle involves transmitting electromagnetic waves that are reflected at the interfaces between structural layers due to differing dielectric constants. Information on internal road conditions is derived from the parameters of incident and reflected waves, including energy, amplitude, and time [78,79], as illustrated in Figure 8.

Currently, 2D and 3D ground-penetrating radar (GPR) devices are commonly employed for distress detection. Their data images are shown in Figure 9, and it is evident that 2D GPR offers the advantages of a lightweight design, high detection efficiency, and nondestructive testing. However, its limitation to a single longitudinal profile per scan may cause the oversight of secondary distress, as hidden defects like interfacial voids at repair zones and unfilled cracks often exhibit asymmetric spatial distributions. While

sharing identical operating principles, 3D GPR utilizes multichannel antenna arrays to comprehensively visualize internal pavement structures, enabling the precise mapping of distresses' planar coordinates and depth profiles. Achieving full cross-sectional coverage of a single lane in a single pass, it demonstrates broader applicability than 2D GPR.

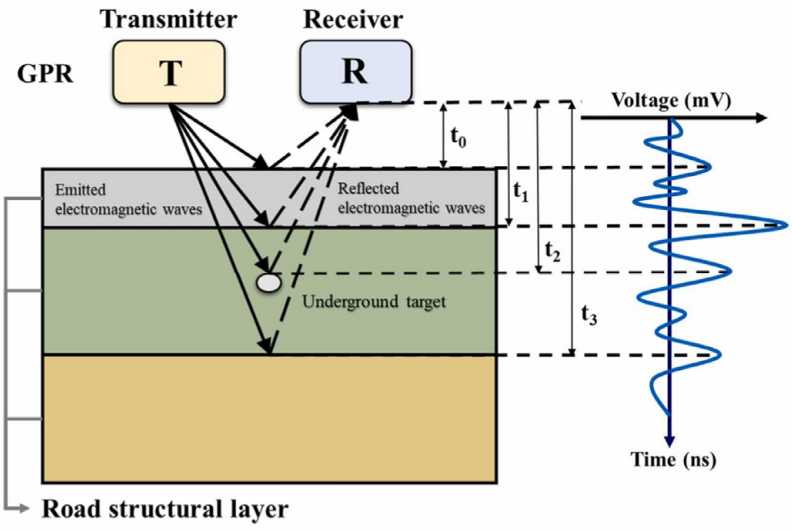


Figure 8. The GPR working principle [80].

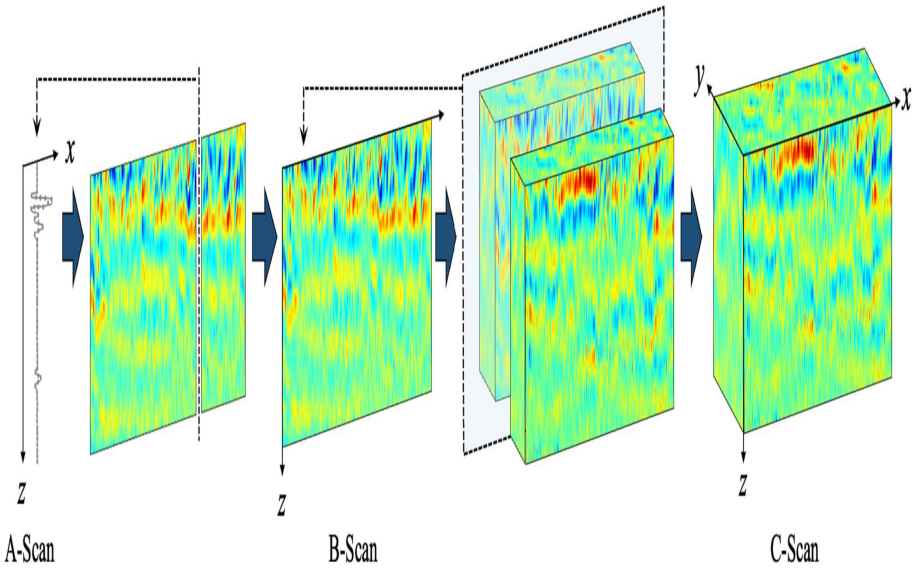


Figure 9. Data collection and display of GPR [81].

For GPR-acquired data images, deep learning and algorithmic enhancements progressively intensify distress signatures and improve recognition accuracy within radargrams. Dou et al. [82] employed unsupervised machine learning to extract RSD features, segregating the regions of interest (ROIs) from the backgrounds, enabling distress identification via hyperbolic signatures. Yao et al. [83] developed the MC-YOLOv4 algorithm, demonstrating significant improvement in mean detection accuracy compared to conventional SD, YOLOv4, and YOLOv5-S algorithms. The Hough transform, a classical geometric shape detection algorithm, is widely utilized in GPR pavement distress detection. Harkat et al. [84] applied modified Hough transform methods to detect void-induced hyperbolas. However, detection accuracy was substantially compromised by water, material properties, and electromagnetic interference, obscuring the hyperbolic signatures of RSDs and impeding precise identification.

GPR enables the detection of internal cracks, moisture damage, and interlayer bonding conditions in pavements. The wavefield characteristics of cracks are typically influenced by filler materials, crack types, and the conductivity of the surrounding media [85]. Consequently, the dielectric contrast between grouting materials and original pavement facilitates precise crack localization. When electromagnetic interference traverses the cracks, diffracted wave amplitudes from the crack tips slightly exceed those from reflective cracks at interfaces between asphalt surface courses and semi-rigid base courses [86]. This amplitude differential provides critical indicators for determining crack depth profiles and classification. Yang et al. [87] established a heterogeneous multiphase discrete medium model for asphalt pavements, based on the significant dielectric constant differences between layered materials, demonstrating GPR's feasibility in detecting interlayer bonding conditions. GPR antennas are categorized as ground-coupled or air-coupled types. Marecos et al. [88] investigated ground-coupled and air-coupled GPR at varying antenna frequencies, revealing superior defect identification capability with 1.0 GHz air-coupled GPR (Figure 10). Wang et al. [89] found that lowering the center frequencies enhances the detection of hidden cracks within asphalt pavement layers.

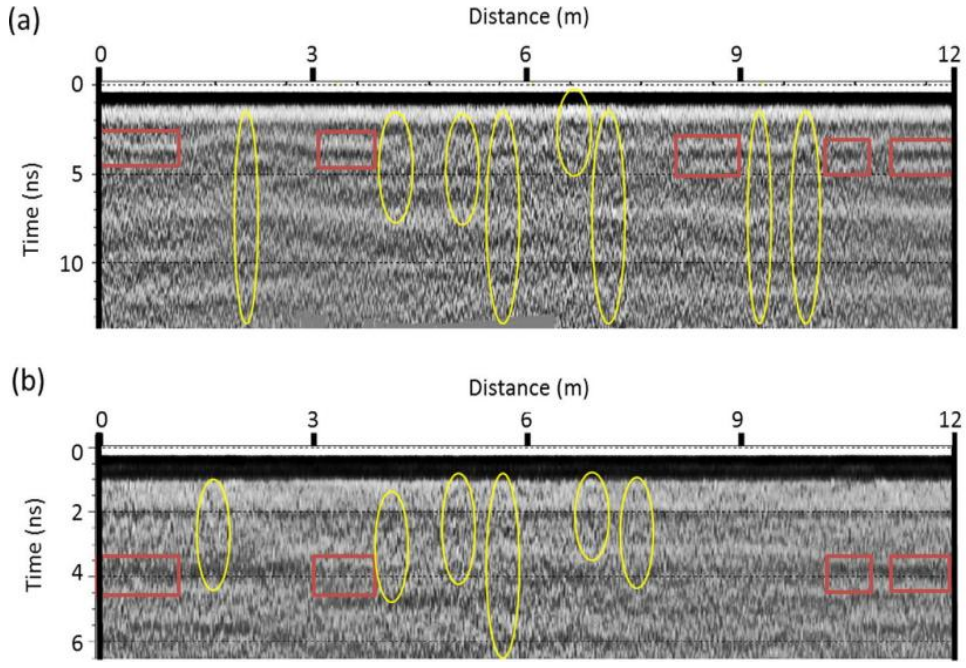


Figure 10. GPR data obtained with the 1.0 GHz (**a**) and the 2.3 GHz (**b**) ground-coupled antennas [88].

Comprehensive analysis indicates that ground-penetrating radar (GPR), as a critical tool in nondestructive testing, has achieved large-scale implementation in road engineering inspections. Leveraging electromagnetic wave reflection principles, this technology demonstrates significant advantages in detecting deep structural distress, such as damage within the asphalt concrete layers and base courses. However, limitations persist in identifying micro-cracks within shallow repair zones (<5 cm depth), primarily being constrained by signal resolution and clutter interference. To address these technical limitations, future research should focus on the deep integration of computer vision technology, optimizing convolutional neural networks and transfer learning algorithms while expanding training dataset volumes to enable the intelligent recognition of millimeter-scale cracks. This approach will provide more reliable quantitative support for pavement maintenance decision-making.

4.1.2. Infrared Thermography (IRT)

The captured signals are subsequently processed to reconstruct the temperature distribution across the asphalt pavement surface. This enables the inspection of asphalt concrete [90]. This technique overcomes the spatial resolution limitations inherent in conventional detection methods. It establishes a novel digital diagnostic approach for road engineering applications.

Infrared thermography, as a representative nondestructive testing technique, enables the accurate identification of subsurface defects, surface cracks, and interlayer bonding conditions [91]. Vyas et al. [92] investigated its efficacy for detecting bonding conditions in asphalt pavements, demonstrating a thermal contrast difference exceeding 0.5 °C between debonded and bonded areas, with the optimal detection period being identified as in the evening to early morning. However, this method does not enable the determination of defect depth localization, and the maximum detection depth is limited to 5 cm. Singla et al. [93] conducted nondestructive collaborative monitoring of repair healing processes for thin concrete cracks (width of $\leq$0.5 mm) using ultrasonic technology and infrared thermography, validating the feasibility of both techniques in assessing sealed-crack repair effectiveness. For the severity classification of cracks, the boundaries primarily serve as demarcation criteria, leveraging the color differences between cracks and their surroundings [94]. As illustrated in Figure 11, three image types (visible light, infrared, and fused images) of identical subjects were collected. Du et al. [95] employed infrared thermography to capture thermal images of pavement surfaces. Utilizing grayscale and temperature information on the cracks within the images, they established a relationship between temperature differentials and crack propagation extent, providing critical guidance for the preventive maintenance of asphalt pavements. Golrokh et al. [96] integrated infrared thermography with high-resolution visual imaging and real-time image processing techniques, achieving the quantitative characterization of geometric features and the damage severity of surface cracks in asphalt pavements.

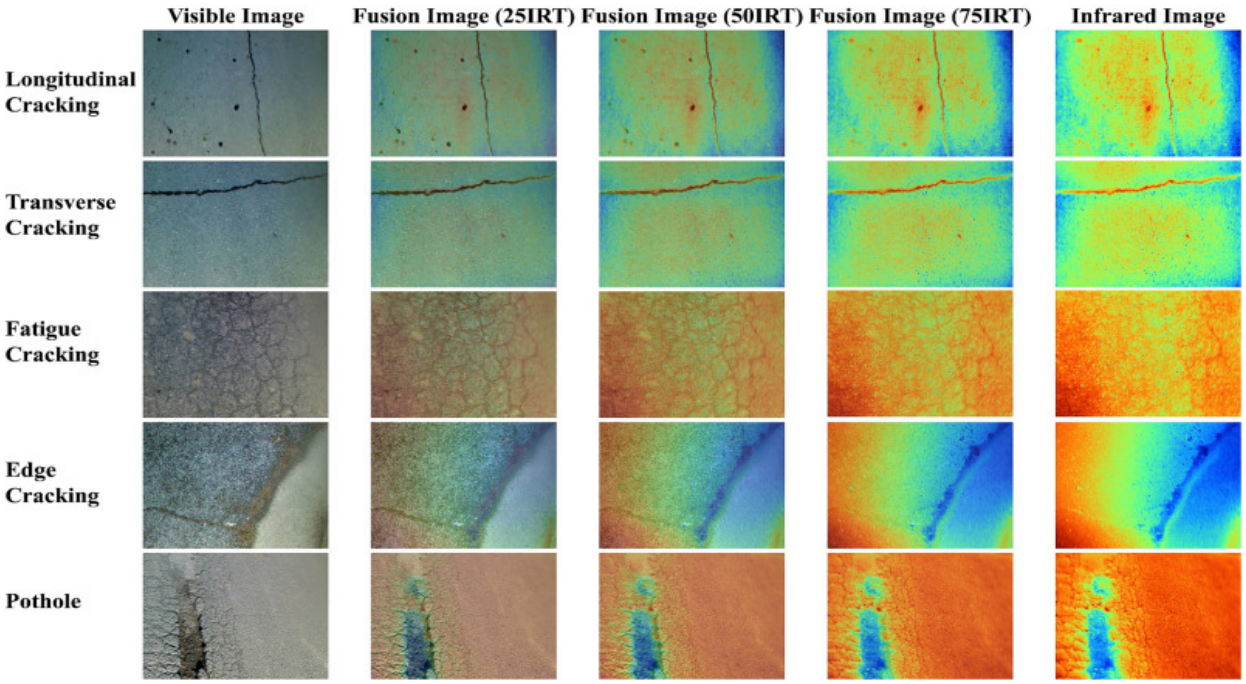


Figure 11. Principal infrared thermal imaging instrument temperature measurement diagram [97].

In summary, infrared thermography demonstrates significant technical advantages in efficient detection and the quantitative assessment of pavement surface conditions, leveraging its non-contact nature and full-field detection capability. For shallow surface damage, this technique exhibits commendable identification efficiency and accuracy. However, environmental factors, such as temperature and humidity variations, and ultraviolet radiation, may compromise thermal imaging results, necessitating further calibration and compensation. Integrating rapidly advancing computer algorithms and deep learning technologies to enhance thermal image features, enable pattern recognition, and expand training dataset volumes could substantially improve damage identification accuracy under complex environmental conditions.

4.1.3. Ultrasonic Testing (UT)

Ultrasonic testing technology exhibits significant advantages in engineering inspection due to its accessible signal acquisition, biological compatibility, and broad applicability. Compared with conventional acoustic waves, ultrasonic waves demonstrate enhanced penetration capabilities, which can be attributed to their shorter wavelengths, enabling the effective detection of deep-layer materials. Leveraging these technical strengths, ultrasonic testing has emerged as a critical methodology in nondestructive evaluations for road engineering, with extensive applications in subgrade compaction assessment, pavement interlayer bonding inspection, and the identification of internal material defects [98].

Principles of ultrasonic testing: A high-frequency elastic wave is generated in the material or structure by an ultrasonic transducer. During propagation through the medium, this wave undergoes reflection and scattering upon encountering defects or impurities. The altered wave is subsequently captured by a receiving transducer [99], as illustrated in Figure 12. By analyzing signal characteristics—including propagation time, frequency, and amplitude—correlations are established between these parameters and material properties such as compaction degree, void content, and strength. This enables the determination of internal defects within the material [100].

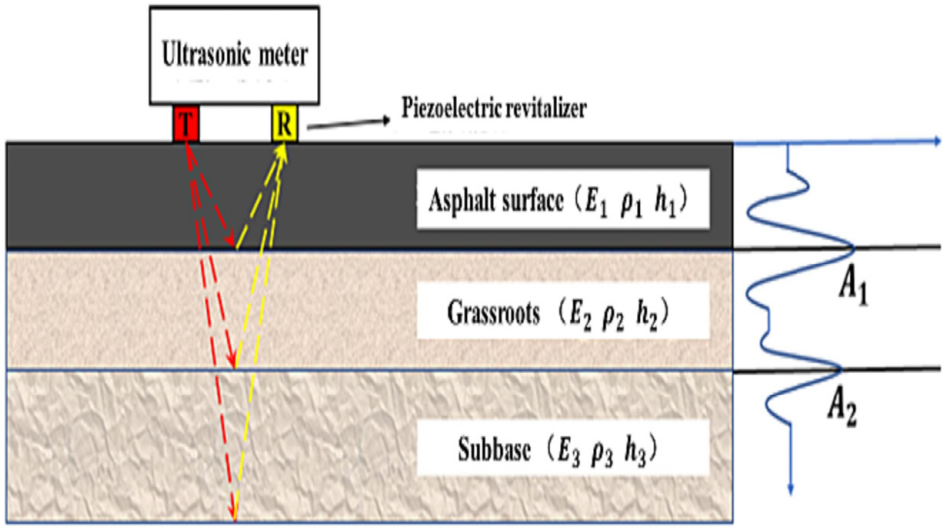


Figure 12. Principles of ultrasonic detection of asphalt pavement damage [99].

Challenges in the ultrasonic testing of asphalt mixtures primarily involve optimizing transducer selection and frequency parameters according to their material properties. This necessity arises from wave energy attenuation during their propagation through media with heterogeneous microstructures. Franesqui et al. [101] simulated cracks in asphalt concrete specimens and evaluated the crack depths ultrasonically, as illustrated in Figure 13.

In a separate study, Franesqui et al. [102] also demonstrated the feasibility of ultrasonic techniques for detecting and quantifying surface crack depths in asphalt pavements through laboratory and in situ testing under varying temperature conditions. Zhang et al. [103] demonstrated that ultrasonic wave propagation exhibits sufficient sensitivity to both crack depth and location. Models with identical crack sizes in different positions show distinct displacement responses, while models with different crack sizes in identical positions exhibit reduced displacement as crack dimensions increase. This characteristic enables the detection of incipient microcracks at specific locations. Li et al. [104] conducted a comparative analysis of ultrasonic and electromagnetic waves through numerical simulations, examining four key aspects: inspection principles, wave equations, medium characteristics, and propagation attenuation. The results demonstrate that the ultrasonic method offers high resolution (~1 cm) but has limited detection depth (0.8–1.2 m) and requires smooth pavement surfaces. Conversely, GPR detects subsurface defects efficiently without the need for direct contact, yet it exhibits lower resolution (~3 cm) and greater susceptibility to electromagnetic interference.

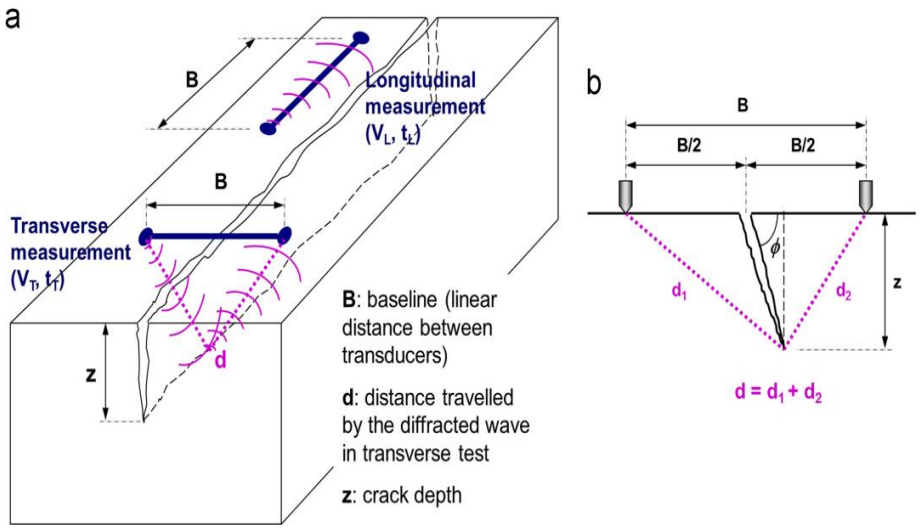


Figure 13. (**a**) Diagram of longitudinal and transverse ultrasound measurements with a surface-breaking crack; (**b**) assumed theoretical wave propagation model in the transverse test [101].

In summary, ultrasonic testing represents one of the most promising nondestructive evaluation methodologies. While rapid advancements in modern technology have significantly enhanced the precision and resolution of road-based ultrasonic inspection systems, current research predominantly focuses on laboratory validation using specimens with singular defect types (e.g., cracks or voids). Field applications for asphalt pavement assessment remain limited. Practical challenges arise from surface roughness, contaminants, and other site-specific factors that adversely affect ultrasonic measurements. Future studies should quantify the influence of these variables to enable a paradigm shift from qualitative defect assessment to precise quantitative analysis. Integrating ultrasonic testing with complementary techniques such as ground-penetrating radar can yield synergistic effects ("1 + 1 > 2"), establishing a multi-source data integration framework. Implementing this approach in field conditions will substantially improve the accuracy and reliability of subsurface distress diagnosis in pavement structures.

A comparison of technical characteristics is presented in Table 3.

Table 3. Comparison of three nondestructive testing techniques.

Nondestructive Testing Technique	Detection Principle	Detection Targets	Detection Depth	Technical Advantages
GPR technology [82–88]	Dielectric Constant	Density, thickness, void content, and subsurface hidden defects	3–4 m	High accuracy and speed for density/thickness/hidden defect detection, yet it is model-dependent.
Infrared thermal imaging technology [92–97]	Infrared Radiation	Temperature segregation, compaction uniformity, pavement water seepage, surface cracks, etc.	2–3 m	Enables intuitive and precise long-term pavement condition monitoring, with particular advantage in detecting incipient micro-cracks within surface layers.
Ultrasonic testing technology [101–105]	Elastic Wave Reflection	Hidden cracks, interlayer bonding, moisture content, etc.	0.8–1.2 m	Effective internal damage inspection with low environmental constraints, suitable for complex pavement structures.

4.2. Active Sensing Technologies for Sealed-Crack Repair Failure Detection

Recent proposals by road engineering professionals envision intelligent transportation systems (ITSs) that effectively integrate advanced information technologies, data communication transmission technologies, and sensor technologies into comprehensive ground transportation management frameworks. This integration aims to achieve intelligent maintenance throughout the entire pavement lifecycle. As a critical enabler of this objective, intelligent monitoring sensor systems provide real-time feedback on key state parameters, including internal stress–strain values, temperature, and humidity within pavement structures. This capability allows maintenance personnel to accurately identify incipient damage and implement timely interventions, thereby significantly reducing maintenance costs while preventing the progression to severe defects that compromise pavement service performance [105].

Current traffic sensors are primarily categorized as external-mounted and embedded types. External-mounted sensors (e.g., radar detectors, ultrasonic sensors, and infrared detectors) are subject to multiple constraints, including high equipment costs and an inability to monitor pavement stress states. Embedded sensors (e.g., magnetometers and induction coils) exhibit material property mismatches with pavement matrices. Under sustained traffic loading and environmental exposure, stress concentration develops at sensor–pavement interfaces [106], ultimately causing device failure and signal loss.

With the rapid advancement of nanotechnology and materials science, novel sensing materials and auxiliary facilities continue to emerge. Among these, flexible pressure sensors represent a relatively mature technology with an extensive application scope. Based on several distinct sensing mechanisms, they primarily include piezoresistive, piezoelectric, and capacitive types. Compared with the other two types, piezoresistive sensors are widely implemented due to their structural simplicity and signal processability [107,108].

4.2.1. Piezoresistive Materials for Active Failure Detection

Piezoresistive sensors operate by utilizing the piezoresistive effect. When subjected to pressure, the relative distances between internal conductive fillers alter, inducing the restructuring of conductive networks—either through the formation of new conductive pathways or the disruption of existing ones. These dynamic microstructural changes cause significant variations in the bulk resistivity of conductive composites, thereby converting pavement stress/strain states into measurable resistance variations [109,110]. Building

on this principle, such sensors enable the monitoring of microcrack formation in pavements. Research confirms that crack initiation and propagation disrupt internal conductive networks within mixtures, consequently increasing their electrical resistance. Real-time changes in this resistive response actively detect crack generation, establishing a novel approach for preventive pavement maintenance [111,112].

Typically, as illustrated in Figure 14, resistance variations in asphalt-based piezoresistive materials under piezoresistive effects result from three concurrent mechanisms [113–115]:

(a) Proximity effect, induced by the convergence or separation of conductive particles under compressive/tensile stresses;
(b) Micro-crack effect, caused by the fracture of conductive pathways due to micro-crack formation, elevating electrical resistance;
(c) Conductive path misalignment/restructuring effect, hindered by the viscoelastic behavior of asphalt mixtures, preventing the full restoration of conductive paths to initial states upon unloading.

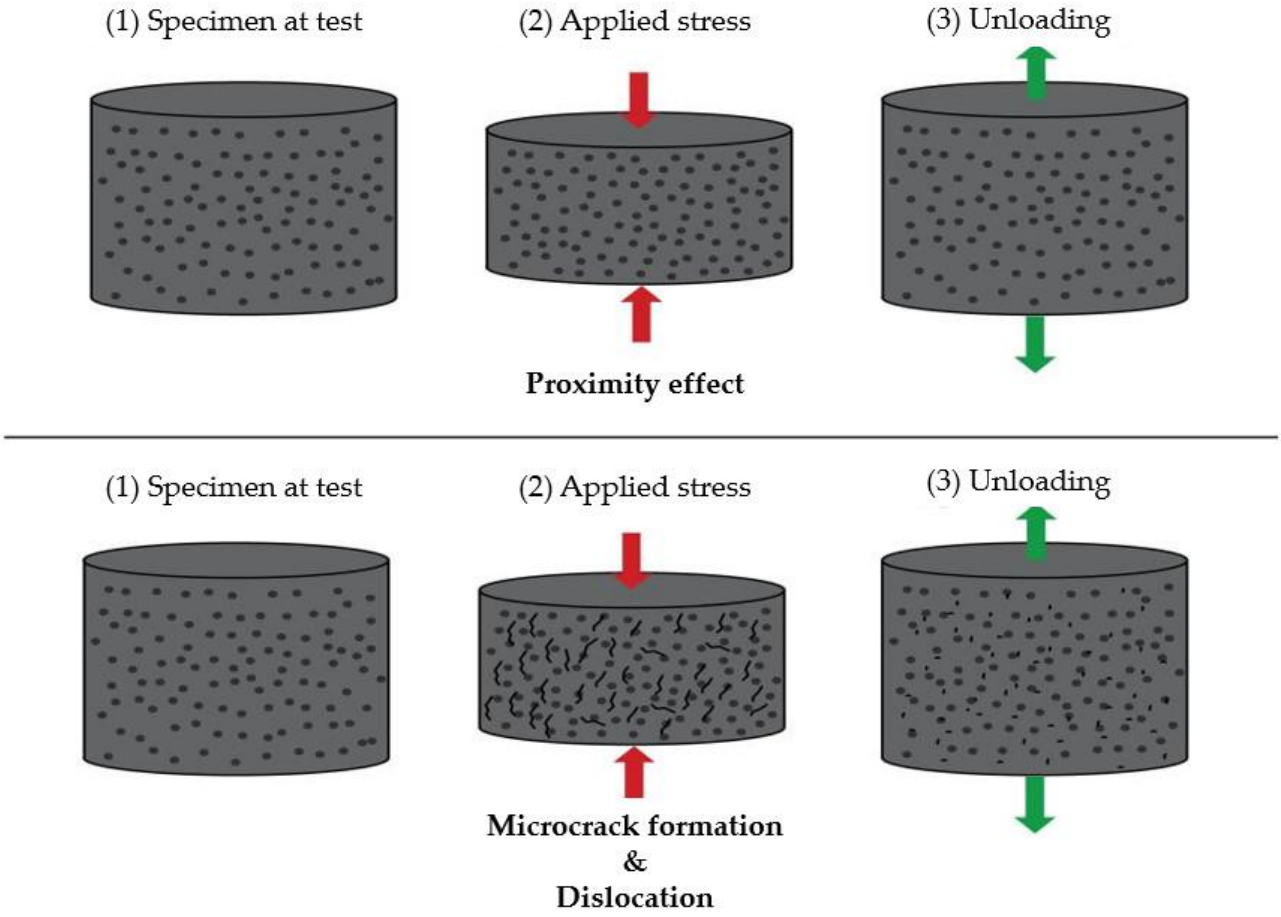


Figure 14. Piezoresistive mechanism of conductive asphalt mixtures [113].

Simultaneously, the formation and evolution mechanisms of conductive pathways are influenced by the type and concentration of conductive fillers. Previous research demonstrates that when the filler concentration reaches a critical value, the composite transitions from an insulator to a conductor as conductive pathways form between the filler particles. Further increases in filler concentration cause the material's resistivity to plummet by several orders of magnitude. Ruschau et al. [116] established that continuous conductive networks emerge within the material at precisely this critical concentration; alterations to these networks under external loading induce corresponding changes in

bulk resistance. This critical concentration is termed the percolation threshold. García et al. [117] further revealed through physical modeling that maintaining filler concentration near this threshold significantly enhances sensor sensitivity. Liang et al. [118] investigated the resistivity in carbon nanotube/epoxy composites across varying concentrations, as illustrated in Figure 15. The resistivity of unstressed nanocomposites plummets with increasing CNT content, plateauing beyond 0.80 wt.% CNTs. Consequently, conductive filler concentration constitutes a pivotal factor in regulating sensor performance.

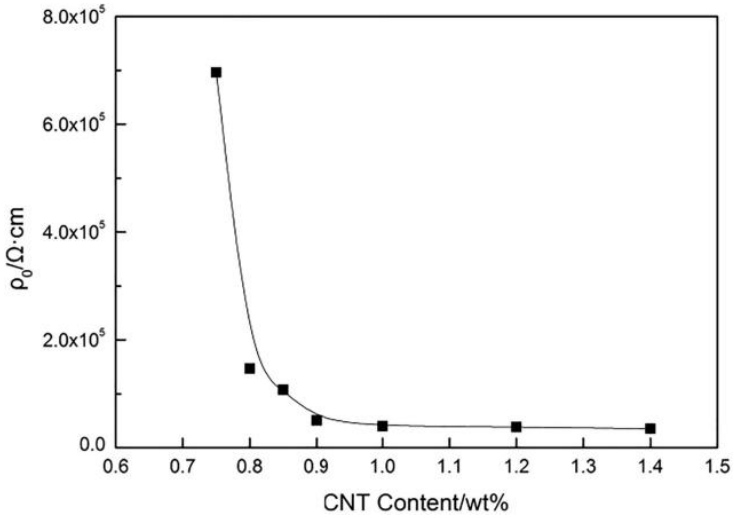


Figure 15. Electrical resistivity of CNT/epoxy composites [118].

Piezoresistive materials are typically fabricated from a single material or composites incorporating graphene, carbon nanotubes (CNTs), carbon fibers, etc. While cement-based piezoresistive materials have been extensively studied for use in concrete pavements, their application in asphalt pavements remains limited. This limitation is primarily attributed to the significant differences in mechanical properties between concrete and asphalt pavements, compounded by the elevated viscosity of asphalt. High viscosity promotes the agglomeration of conductive fillers during incorporation, preventing the formation of continuous conductive networks. As shown in Figure 16, the SEM images reveal the dispersion states of CNTs after high-speed shearing. The micrographs demonstrate the favorable dispersion of processed CNTs with only minor agglomerates, contrasting markedly with the pre-dispersion agglomeration pattern [111].

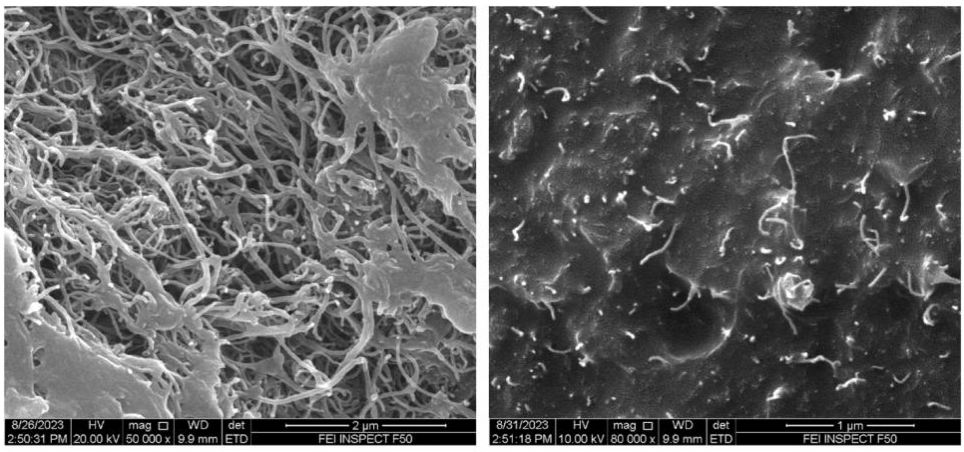


Figure 16. SEM image of carbon nanotube-modified epoxy resin before and after treatment [111].

As a way to address the application challenges of piezoresistive materials in asphalt pavements, tailored composite materials offer viable solutions. As summarized in Table 4, sensors fabricated from diverse material systems demonstrate distinct performance characteristics. The sensitivity of strain sensing can be evaluated via the fractional change in resistance (FCR) or gauge factor (GF), with conventional metals exhibiting a GF of approximately 2.

$$FCR = \frac{R - R_0}{R_0} = \frac{\Delta R}{R_0} \quad (2)$$

$$GF = \frac{\Delta R / R_0}{\varepsilon} = \frac{FCR}{\varepsilon} \quad (3)$$

Table 4. Sensors based on diverse conductive fillers.

Literature	Conductive Filler	Matrix	Optimum Dosage	Percolation Threshold/Region	Sensitivity Evaluation Metric		Sensor Durability Validation
					GF	FCR	
[118]	CNT/EP	Asphalt	0.8 wt.% CNTs	Graphene percolation region: 2%–6%. CNT percolation region: 2%–5%. Steel fiber percolation threshold: 1.2%. Carbon fiber percolation threshold: 1%–6%.	26.04	-	fatigue tensile test
[119]	CNTs-GNP/EP	Asphalt	0.5 wt% CNTs + 0.3 wt.% GNP/Ep		13.42	-	Bending strain test
[120]	CF	Asphalt Concrete	CF mixture ratio (3 mm:6 mm:9 mm): 2:6:2, 5.5 wt.% CF		40.40	51%	Piezoresistive response under vehicle loading
[121]	SF/CF/CNT	Cement	0.5 wt.% CNTs		33.40	7.81%	Bending fatigue life test
[122]	Graphene/Cement	Cement	0.5 wt.% Graphene		149.5	14.2%	Cyclic compression test

Based on the above data, piezoresistive sensors have demonstrated their preliminary feasibility as one of the key technologies used for enabling intelligent transportation systems. However, existing research predominantly relies on the performance testing of laboratory specimens. As noted in Ref. [108], a phenomenon exists in piezoresistive mixtures where the resistance change lags behind the strain response, with the lag time affected by factors such as temperature and humidity. Therefore, a deeper elucidation of the sensing mechanism is required to further evaluate sensor performance. In practical engineering applications, sensor placement locations are more diverse, their stress states become more complex, and their impact mechanisms on the fatigue life of the structure are more intricate. Future research could combine laboratory experiments with numerical simulations to optimize the geometric dimensions and placement strategies of the sensors.

4.2.2. Piezoelectric Materials for Active Failure Detection

Cement concrete exhibits less sensitivity to temperature variations. Consequently, the propagation of signals from embedded piezoelectric sensors within concrete remains relatively stable, which simplifies and enhances the efficiency of damage monitoring. In contrast, asphalt concrete is a typical temperature-dependent material. Its mechanical properties and air void content change significantly with temperature, which, in turn, affects its signal propagation characteristics [123]. Zhao et al. [124] analyzed the interaction between piezoelectric sensors and asphalt pavements using finite element modeling. Their results demonstrate that the sensor's energy conversion efficiency decreases with increasing

embedment depth and surface layer modulus. The reductions were approximately 13 V/cm and 12 V/200 MPa.

The operating principle of piezoelectric sensors can be represented by an equivalent circuit, commonly known as the Van Dyke model [125], as illustrated in Figure 17. Simply put, under traffic loading, piezoelectric sensors deform. This deformation causes a relative displacement of the positive and negative charge centers within the core material (e.g., piezoelectric ceramic (PZT)), generating polarization charges and consequently creating a voltage difference (i.e., voltage) through the piezoelectric effect. Simultaneously, damage within the pavement structure alters the resulting strain field and consequently affects the generated voltage signal [126,127]. Thus, by analyzing the patterns of strain or voltage signals in response to traffic loading, it is possible to monitor barely perceptible damage within the pavement.

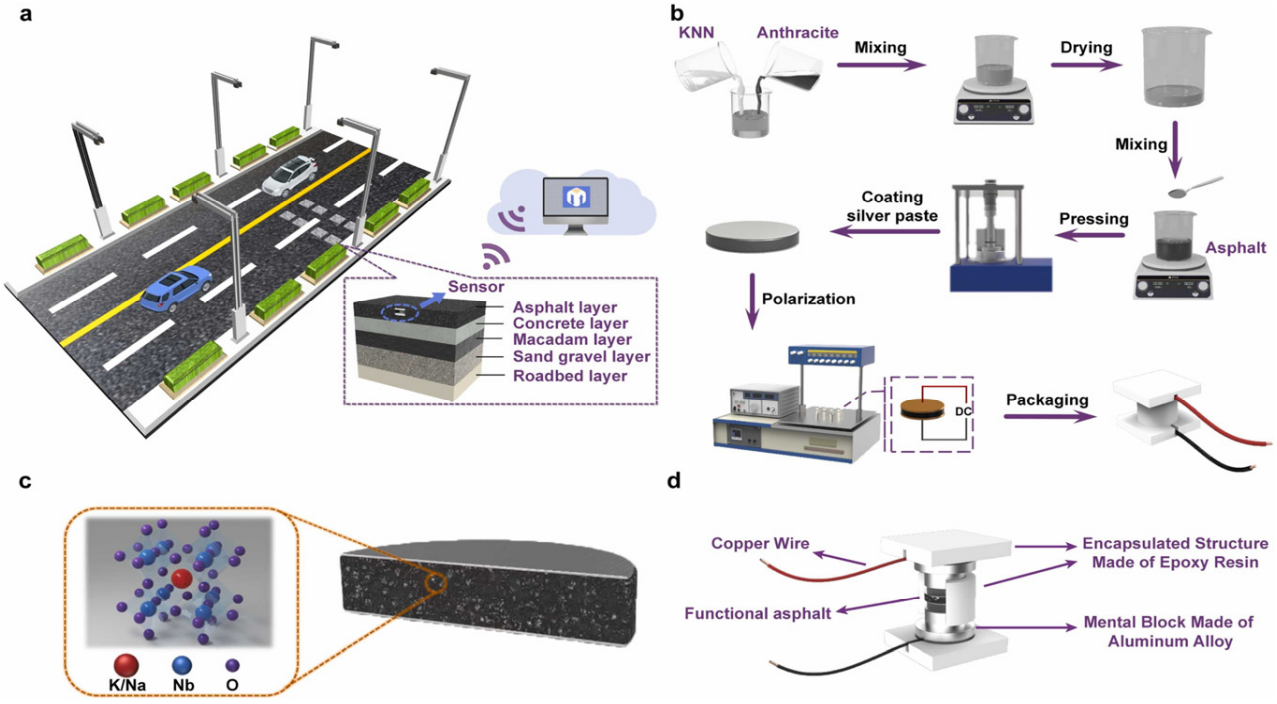


Figure 17. Schematic of the fabrication strategy for the asphalt-based sensor and its application (**a**) Road application diagram. (**b**) Fabrication strategy for the asphalt-based sensor. (**c**) Schematic working principle of the functional asphalt. (**d**) An exploded view of sensor packaging [128].

Traditional wired sensors [129–131] present limitations in their installation and maintenance. Furthermore, processing the large volumes of data generated by dense arrays of wired sensors presents significant challenges and is costly [132]. To overcome these drawbacks, many researchers have turned to wireless sensors as a promising alternative, which are cost-effective and easier to maintain. However, the practical deployment of wireless sensors necessitates either a self-powered design or access to a sustainable power source [133]. As presented in Table 5, the feasibility of using self-powered wireless piezoelectric sensors for pavement crack detection has been investigated.

Table 5. Research results on wireless piezoelectric sensors.

References	Piezoelectric Materials	Pavement Type	Research Objectives	Result
[134]	SWS	Asphalt Concrete	Fatigue cracking at asphalt concrete bottom due to excessive tensile strain.	Both changes in μ and σ of the CDF can locate damage. σ primarily indicates damage severity.
[135]	SWS	Asphalt Concrete	Bottom-up cracking caused by excessive strain at asphalt concrete base.	Percentage of voltage/strain droppage is a reliable indicator of damage progression. The gate number and activation effectively reflect damage severity.
[136]	PZT + PVDF	Asphalt	Monitoring hidden damage in asphalt pavements (e.g., microcracks).	Acoustic attenuation coefficient obtained from the self-powered damage-detection aggregate (SPA) decreases with increasing crack width in asphalt pavements (Figure 18).
[137]	PZT + EP	Cement	Depth of crack propagation and localization of crack damage in concrete beams.	The output signal amplitude from piezoelectric sensors effectively determines the development of macroscopic cracks and locates crack positions in concrete (Figure 19).

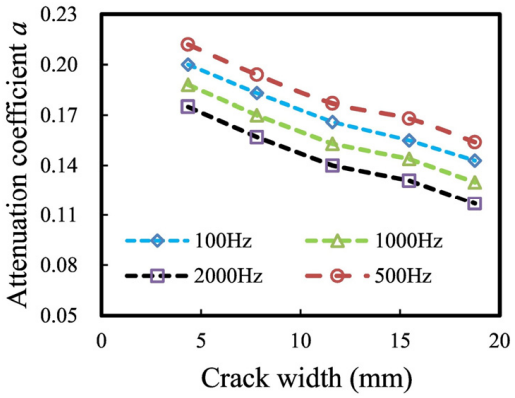


Figure 18. Relationship between the attenuation coefficient and crack width [136].

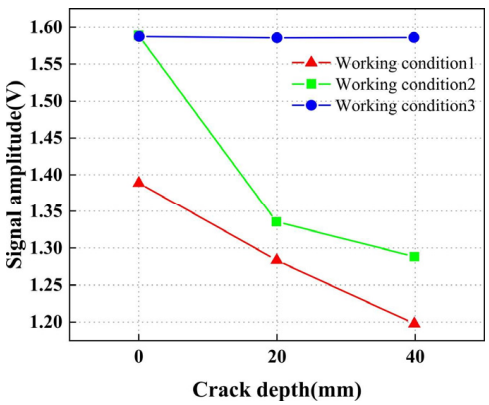


Figure 19. Graph of the average signal amplitude variation under different damage depths for each working condition [137].

In summary, the current application of piezoelectric sensors primarily relies on finite element simulations and laboratory tests. Their feasibility for the active detection of pavement cracks has been well validated. However, previous researchers [138] have reported a significant decline in the power output of piezoelectric energy harvesters after one year of service. Therefore, a comprehensive investigation into the mechanical properties and fatigue/aging behavior of piezoelectric sensors is required. Furthermore, given the significant modulus mismatch between piezoelectric materials and asphalt/concrete pavements, and considering the coupled effects of multiple environmental factors, future research should prioritize investigating the influence of environmental conditions and seasonal variations on the performance of piezoelectric sensors.

5. Conclusions

This comprehensive review has systematically examined the current state of the art in terms of asphalt pavement crack sealing technologies, encompassing material innovations, failure mechanisms, and detection methodologies. Crack sealing technology has undergone significant advancement from the conventional bituminous materials to sophisticated polymer-modified and nanocomposite systems. These developments have enabled substantial improvements in the critical performance parameters, including enhanced high-temperature stability, superior low-temperature ductility, and strengthened interfacial bond characteristics. The integration of nanomaterials, particularly nanosilica- and carbon-based additives, has proven effective in addressing the traditional limitations of thermal susceptibility and adhesive degradation.

Multiple failure modes have been identified and characterized, with interfacial bond failure emerging as the predominant mechanism compromising long-term performance. Environmental stressors, including thermal cycling, UV radiation exposure, and moisture infiltration, coupled with construction variability, constitute the primary drivers of premature sealant failure. To extend pavement service life, the timely detection of pavement conditions and the effective treatment of emerging distress are essential.

Developments include biomimetic self-healing mechanisms incorporating microvascular networks and shape-memory polymers to achieve autonomous crack repair capabilities. Investigations have been made into hybrid nanomaterial systems combining mechanical reinforcement, thermal regulation, and sensing capabilities within single-material platforms. Particular attention should be directed toward graphene-based composites and smart nanoparticle systems.

Future research directions are proposed to guide the application of crack sealing materials in asphalt pavement crack rehabilitation. Crack sealing technology will evolve toward full-cycle intelligent development, encompassing material innovation, process optimization, and monitoring integration, with future research recommended to focus on the following strategic directions:

(1) Optimization of sealing materials and construction technologies:
   - Development of self-healing microcapsule materials.
   - Application of bio-based modified materials.
   - Integration of piezoresistive materials into sealants.
   - Emphasizing crack pretreatment (cleaning and drying).
   - Implementing material preheating and precision temperature control during sealing and grouting.

(2) Interfacial bonding failure mechanisms:
   - Molecular dynamics simulations, as used to reveal the failure mechanisms.

- Combined natural exposure testing and laboratory simulations for comprehensive mechanism analysis.

(3) Post-repair detection methods:

- For ground-penetrating radar technology, future research should advance antenna array configurations with multichannel and multi-polarization designs, enhance detection accuracy and pretrained models through deep learning and algorithmic optimization, and optimize antenna selection based on distress characteristics and location—a context where ground-coupled antennas excel at detecting surface cracks and delamination, while air-coupled antennas offer superior precision for internal pavement defects.
- For infrared thermography technology, future trends include the integration of unmanned platforms (e.g., unmanned aerial vehicles), the implementation of AI-powered intelligent distress identification and analysis, and the synergistic processing of multi-source data with complementary 3D information.
- For ultrasonic testing technology, future research should advance toward miniaturization, enhanced efficiency, and real-time monitoring.
- The hybridization of three complementary passive detection techniques can be used to overcome individual limitations.

These research directions will contribute to transformative improvements in pavement infrastructure sustainability, maintenance efficiency, and lifecycle cost optimization. The integration of intelligent materials, predictive modeling, and autonomous monitoring systems represents a paradigm shift toward proactive infrastructure management, with potential applications extending beyond pavement engineering to broader civil infrastructure domains.

Author Contributions: W.M.: data analysis, methodology, and writing—original draft; P.L.: data analysis, methodology, and formal analysis; S.L.: conceptualization, methodology, project administration, and writing—review and editing; H.W.: conceptualization and writing—review and editing. All authors have read and agreed to the published version of the manuscript.

Funding: This work was supported by the Natural Science Foundation of Jiangsu Province of China (BK20220419), China Postdoctoral Science Foundation (2023M741454), and the Jiangsu Provincial Double-Innovation Doctor Program (JSSCBS20220685).

Institutional Review Board Statement: Not applicable.

Informed Consent Statement: Not applicable.

Data Availability Statement: All data, models, and codes generated or used in this study are included in the submitted manuscript.

Acknowledgments: The authors would like to express their sincere gratitude to all funding organizations that supported this research.

Conflicts of Interest: The authors declare no conflicts of interest.

References

1. Wang, W.; Wang, L.; Xiong, H.; Luo, R. A review and perspective for research on moisture damage in asphalt pavement induced by dynamic pore water pressure. *Constr. Build. Mater.* **2019**, *204*, 631–642. [CrossRef]
2. Li, X.; Ye, J.; Zhou, Z.; Yang, L.; Wang, S.; Diab, A. Preparation and performance of an asphalt pavement sealant with waterborne epoxy resin. *Constr. Build. Mater.* **2022**, *350*, 128827. [CrossRef]
3. Soliman, H.; Shalaby, A.; Kavanagh, L. Performance evaluation of joint and crack sealants in cold climates using DSR and BBR tests. *J. Mater. Civ. Eng.* **2008**, *20*, 470–477. [CrossRef]

4. Xu, T.; Huang, X. Investigation into causes of in-place rutting in asphalt pavement. *Constr. Build. Mater.* **2012**, *28*, 525–530. [CrossRef]
5. Minhoto, M.J.; Pais, J.C.; Pereira, P.A. The temperature effect on the reflective cracking of asphalt overlays. *Road Mater. Pavement Des.* **2008**, *9*, 615–632. [CrossRef]
6. Wang, S.; Jia, Y.; Li, Z.; Zhou, Z.; Gao, Y.; Huang, X.; Wei, H.; Guan, S. Evaluating the effect of aging on adhesion for hot-poured road sealants through a modified adhesion test. *Constr. Build. Mater.* **2022**, *347*, 128576. [CrossRef]
7. Sawalha, M.; Ozer, H.; Al-Qadi, I.L.; Xue, H. Development of a modified adhesion test for hot-poured asphalt crack sealants. *Transp. Res. Rec.* **2017**, *2612*, 85–95. [CrossRef]
8. Wu, S.; Liu, Q.; Yang, J.; Yang, R.; Zhu, J. Study of adhesion between crack sealant and pavement combining surface free energy measurement with molecular dynamics simulation. *Constr. Build. Mater.* **2020**, *240*, 117900. [CrossRef]
9. Zhi, S.; Gun, W.W.; Hui, L.X.; Bo, T. Evaluation of fatigue crack behavior in asphalt concrete pavements with different polymer modifiers. *Constr. Build. Mater.* **2012**, *27*, 117–125. [CrossRef]
10. Zhang, H.; Sheng, X.; Wang, S.; Xu, T. Effects of different modifiers on thermal stability, constituents and microstructures of asphalt-based sealant. *J. Therm. Anal. Calorim.* **2020**, *142*, 1183–1192. [CrossRef]
11. Li, Q.; Sun, G.; Lu, Y.; Meng, Y.; Luo, S.; Gao, L. Effects of warm-mix asphalt technologies and modifiers on pavement performance of recycled asphalt binders. *J. Clean. Prod.* **2021**, *282*, 125435. [CrossRef]
12. Xu, Z.; Jiang, Y.; Xu, T. Pavement property improvement of graphene modified asphalt and its improving mechanism. *J. For. Eng.* **2023**, *8*, 154–160. [CrossRef]
13. Tao, M.; Xu, T. Development and Properties of Bio-Based Rice Oil Microcapsule and Its Dispersibility in Emulsified Asphalt. *J. Ind. Eng. Chem.* **2024**, *131*, 503–513. [CrossRef]
14. Liu, H.; Yan, G.; Zhang, J.; Gan, X.; Liu, S.; Xu, T. Viscosity and toughness of hydrogenated epoxy emulsified asphalt and the road performance of its cold recycled mixture. *J. For. Eng.* **2025**, *10*, 136–143. [CrossRef]
15. Ji, X.; Hu, H.; Sun, Y.; Ji, X. Healing performance of steel fiber reinforced iron tailings hot mix asphalt heated by microwave. *J. Chang. Univ. (Nat. Sci. Ed.)* **2025**, *45*, 1–13.
16. Wang, H.; Xu, T. Piezoelectric Properties and Microstructural Changes of Smart Asphalt-Based Composites Containing Electroactive Polymer and Carbon Black. *Constr. Build. Mater.* **2024**, *444*, 137894. [CrossRef]
17. Liu, L.; Zhang, X.; Xu, L.; Zhang, H.; Liu, Z. Investigation on the piezoresistive response of carbon fiber-graphite modified asphalt mixtures. *Constr. Build. Mater.* **2021**, *301*, 124140. [CrossRef]
18. Guo, S.; Yu, M.; Xu, Z.; Yue, G.; Cai, W.; Tian, P. Study on the Attribute Characteristics of Road Cracks Detected by Ground-Penetrating Radar. *Sensors* **2025**, *25*, 595. [CrossRef]
19. Hashimoto, K.; Shiotani, T. Sonic-IR imaging technique for detection of crack interfaces in cementitious materials. *Constr. Build. Mater.* **2023**, *386*, 131549. [CrossRef]
20. Khazanovich, L.; Velasquez, R.; Nesvijski, E.G. Evaluation of top-down cracks in asphalt pavements by using a self-calibrating ultrasonic technique. *Transp. Res. Rec.* **2005**, *1940*, 63–68. [CrossRef]
21. Zhu, H.; Yang, X. Review of Non-Destructive Testing Technologies for Internal Defects in Asphalt Pavements. *Sci. Technol. Eng.* **2024**, *24*, 10588–10604. [CrossRef]
22. Slabej, M.; Grinč, M.; Kováč, M.; Decký, M.; ŠEDIVÝ, S. Non-invasive diagnostic methods for investigating the quality of Žilina airport's runway. *Contrib. Geophys. Geod.* **2015**, *45*, 237–254. [CrossRef]
23. Ji, X.; Chen, Y.; Li, Y.; Zhou, H. Intelligent recognition and localization of hidden cracks in asphalt pavement based on smartRock. *China J. Highw. Transp.* **2024**, *37*, 408–417.
24. Tong, J. Mechanism Analysis and Prediction of the Rutting and Surface Crack for Asphalt Pavement. Ph.D. Thesis, Southeast University, Nanjing, China, 2022. [CrossRef]
25. Editorial Department of China Journal of Highway and Transport. Academic Research Review on Pavement Engineering in China·2020. *China J. Highw. Transp.* **2020**, *33*, 1–66.
26. Wang, H.; Wu, H.; Wu, Q.; Jin, G.; Zhang, Z. Study on Crack Morphological Characteristics and Cracking Mode of Expressway Crack Based on Field Measured Data. *J. Highw. Transp. Res. Dev.* **2018**, *35*, 28–34. [CrossRef]
27. Li, F.; Shi, X.; Xu, J. Performance Evaluation and Technical Requirements of Asphalt Pavement Crack Seal Band. *J. Beijing Univ. Technol.* **2013**, *39*, 1855–1860. [CrossRef]
28. Wang, S.; Xu, Y.; Liu, M.; Gao, Y.; Jia, Y.; Li, Y.; Chen, Z.; Wei, Z. Dynamic behavior of crack sealant bonding interface in the asphalt pavement crack repair structure under moving vehicle load. *Case Stud. Constr. Mater.* **2023**, *18*, e01821. [CrossRef]
29. *Standard’s JTG 5142-2019*; Asphalt Pavement Maintenance Technical Specifications. Ministry of Transport of the People's Republic of China: Beijing, China, 2019.
30. Yang, D. Research on Repair technology for Asphalt Pavement Cracks in Guizhou Province. Master's Thesis, Nanjing Forestry University, Nanjing, China, 2023. [CrossRef]
31. Li, F.; Xu, J.; Shi, X. Asphalt Pavement Crack Sealing and Filling Technic. *Highway* **2013**, 249–253. [CrossRef]

32. Zhang, M.; Shang, F. Performance Evaluation of Joint Treatment in Gussasphalt Mixtures. *Highway* **2020**, *65*, 188–193.
33. Li, L.; Huang, Y.; Shao, Z.; Ren, D. An experimental investigation on the repairing performance and fatigue life of asphalt pavement potholes with an inclined interface joint. *Front. Mater.* **2021**, *7*, 597523. [CrossRef]
34. Cong, P.; Liu, C.; Zhang, X. Preparation of thermoplastic polyurethane sealant and its adherence properties under various environments. *Compos. Part B Eng.* **2025**, *293*, 112125. [CrossRef]
35. Teng, X.; Wu, P.; Sun, J.; Yang, H.; Zhang, Q. Graphene Oxide-Modified Polysulfide Sealant. *Polym. Mater. Sci. Eng.* **2013**, *29*, 54–57.
36. Ma, B.; Hu, Y.; Liu, F.; Si, W.; Wei, K.; Wang, X.; Kang, X.; Chang, X. Performance of a novel epoxy crack sealant for asphalt pavements. *Int. J. Pavement Eng.* **2022**, *23*, 3068–3081. [CrossRef]
37. Tan, X.; Zhang, J.; Guo, D.; Sun, G.; Zhou, Y.; Zhang, W.; Guan, Y. Preparation, characterization and repeated repair ability evaluation of asphalt-based crack sealant containing microencapsulated epoxy resin and curing agent. *Constr. Build. Mater.* **2020**, *256*, 119433. [CrossRef]
38. Fu, Y.; Wang, S.; Cai, L.; Chen, L. Preparation and Properties of Restructured Polysulfur-Urethane Sealants. *Polym. Mater. Sci. Eng.* **2011**, *27*, 136–139. [CrossRef]
39. Ma, T.; Chen, C.; Zhang, Y.; Zhang, W. Development of Using Crumb Rubber in Asphalt Modification: A Review. *China J. Highw. Transp.* **2021**, *34*, 1–16. [CrossRef]
40. Li, K.; Yan, X.; Ai, T.; Niu, Y.; Jiang, S. Study on properties and application of chloroprene rubber/polyurethane modified asphalt sealant. *Constr. Build. Mater.* **2023**, *406*, 133177. [CrossRef]
41. Gong, Y.; Wu, S.; Zhang, Y.; Pang, Y.; Ma, Y. Investigation of the high-temperature and rheological properties for asphalt sealant modified by SBS and rubber crumb. *Polymers* **2022**, *14*, 2558. [CrossRef]
42. Liu, H.; Wang, Z.; Gao, J.; Xu, X.; Zhou, X.; Jing, H.; Li, J. Property improvement and mechanism of SBS/CR composite modified asphalt sealant with high-polarity EVA modifier. *Constr. Build. Mater.* **2025**, *458*, 139594. [CrossRef]
43. *ASTM D6690-12*; Standard Specification for Joint and Crack Sealants, Hot-Applied, for Concrete and Asphalt Pavements. ASTM International: West Conshohocken, PA, USA, 2012.
44. Hasan, O.; Pranshoo, S.; Seyed, S.Y. Field Validation of Laboratory-Predicted Low-Temperature Performance of Hot-Poured Crack Sealants. *Transp. Res. Rec.* **2014**, *2431*, 57–66.
45. Liu, C.; Wang, H.; Liu, S.; Yang, D.; Xiong, Y. Performance Evaluation of Asphalt-Pavement Crack-Repair Materials. *Materials* **2025**, *18*, 1611. [CrossRef] [PubMed]
46. Li, Q.; Nl, F.; Wang, W. Performance comparison of cracking repairing materials for asphalt pavements. *Highw. Eng.* **2013**, *38*, 33–37.
47. Chen, H.; Ao, F.; He, Q.; Yan, C. Preparation and Performance of Warm Mix Crack Filling Material for Bituminous Pavement in Alpine Region. *J. Civ. Eng. Manag.* **2021**, *38*, 95–100. [CrossRef]
48. Song, L.; Xue, Y.; Xia, H.; Niu, Y. Preparation and properties of SBS/LNBR/CR composite modified asphalt sealant. *Appl. Chem. Ind.* **2023**, *52*, 1630–1636. [CrossRef]
49. Sun, Z.; Li, S.; Zhang, J.; Zeng, Y. Adhesion property of bituminous crack sealants to different asphalt mixtures based on surface energy theory. *Constr. Build. Mater.* **2020**, *261*, 120006. [CrossRef]
50. Wang, W.; He, R.; Chen, Z.; Shi, J.; Xu, L.; Sun, Y. Performance evaluation indicators for asphalt pavement sealants in seasonal frozen region: An experimental study. *Case Stud. Constr. Mater.* **2025**, *22*, e04421. [CrossRef]
51. Li, F.; Zhou, S.; Cai, W.; Du, Y.; Li, L. Laboratory evaluation of short and long term performance of hot-poured sealants. *Constr. Build. Mater.* **2017**, *148*, 30–37. [CrossRef]
52. Lin, C. Research on Sealing Technology and Cracks Investigation for Transverse Cracks of Asphalt Pavement in Large Temperature Difference Region. Master's Thesis, Harbin Institute of Technology, Harbin, China, 2011. [CrossRef]
53. Lai, M. Research on Preparation and Properties of High Performance of Asphalt Pavement Filling Materials. Master's Thesis, Jilin University, Changchun, China, 2016.
54. *Standard’s JTG E20-2011*; Standard Test Methods of Bitumen and Bituminous Mixtures for Highway Engineering. Ministry of Transport of the People's Republic of China: Beijing, China, 2011.
55. Feng, X.; Liang, H.; Peng, C. Preparation and performance of high performance grouting sealant for asphalt pavement in humid and hot areas. *J. Chang. Univ. (Nat. Sci. Ed.)* **2023**, *43*, 11–20. [CrossRef]
56. Li, Y.; Mei, P.; Yuan, H.; Li, F. Viscosity-emperature Characteristics of Asphalt Pavement Hot-applied Sealant. *J. Highw. Transp. Res. Dev.* **2015**, 8–12. [CrossRef]
57. Naskar, M.; Reddy, K.S.; Chaki, T.K.; Divya, M.K.; Deshpande, A.P. Effect of ageing on different modified bituminous binders: Comparison between RTFOT and radiation ageing. *Mater. Struct.* **2013**, *46*, 1227–1241. [CrossRef]
58. Jamal, M.; Giustozzi, F. Enhancing the asphalt binder's performance against oxidative ageing and solar radiations by incorporating rubber from waste tyres. *Constr. Build. Mater.* **2022**, *350*, 128803. [CrossRef]

59. Zhou, Y.; Du, L.; Liu, X.; Zhang, K.; Xu, P.; Zhang, Y. Microscopic performance of modified asphalt based on aging. *Constr. Build. Mater.* **2021**, *279*, 122429. [CrossRef]
60. Li, C.; Xie, X.; Wang, L.; Guo, Y.; Zhang, L.; Xue, Z. Evaluation of the effect of thermal oxygen aging on base and SBS-modified bitumen at micro and macroscales. *Constr. Build. Mater.* **2022**, *324*, 126623. [CrossRef]
61. Camargo, I.G.D.N.; Hofko, B.; Mirwald, J.; Grothe, H. Effect of thermal and oxidative aging on asphalt binders rheology and chemical composition. *Materials* **2020**, *13*, 4438. [CrossRef]
62. Hung, A.M.; Kazembeyki, M.; Hoover, C.G.; Fini, E.H. Evolution of morphological and nanomechanical properties of bitumen thin films as a result of compositional changes due to ultraviolet radiation. *ACS Sustain. Chem. Eng.* **2019**, *7*, 18005–18014. [CrossRef]
63. Hung, A.; Fini, E.H. Surface morphology and chemical mapping of UV-aged thin films of bitumen. *ACS Sustain. Chem. Eng.* **2020**, *8*, 11764–11771. [CrossRef]
64. Enfrin, M.; Giustozzi, F. Chemo-rheological deterioration of bitumen due to UV ageing: Correlations between accelerated UV ageing tests and 1-year outdoor exposure. *Constr. Build. Mater.* **2024**, *449*, 138425. [CrossRef]
65. Li, Y.; Wu, S.; Liu, Q.; Dai, Y.; Li, C.; Li, H.; Nie, S.; Song, W. Aging degradation of asphalt binder by narrow-band UV radiations with a range of dominant wavelengths. *Constr. Build. Mater.* **2019**, *220*, 637–650. [CrossRef]
66. Yang, C.; Cao, L.; Ullah, S.; Dong, Z.; Zhang, X.; Wei, D. Performance evolution and mechanism of asphalt crack sealant under UV aging: A continuity study. *Constr. Build. Mater.* **2024**, *431*, 136539. [CrossRef]
67. Cao, L.; Yang, C.; Dong, Z.; Wang, W.; Yin, H. Aging mechanism of hot-poured sealants for asphalt pavement under natural environmental exposure. *Int. J. Pavement Eng.* **2022**, *23*, 197–206. [CrossRef]
68. Dong, P.; Cao, X.; Tang, B. Research on dynamic stress and excess pore water pressure of asphalt pavement under hydraulic-mechanical coupling. *Heliyon* **2024**, *10*, e26011. [CrossRef] [PubMed]
69. Gao, Y.; Zou, X.; Zhang, T. Review on Damage Mechanism of Asphalt Pavement under Dynamic Water Pressure Effects. *J. China Foreign Highw.* **2018**, *38*, 59–64. [CrossRef]
70. Dong, Z.; Tan, Y.; Cao, L.; Zhong, Y. Research on pore pressure with in asphalt pavement under the coupled moisture-loading action. *J. Harbin Inst. Technol.* **2007**, *39*, 1614–1617. [CrossRef]
71. Chen, W.; Wang, Z.; Guo, W.; Dai, W. Measurement and evaluation for interbedded pore water pressure of saturated asphalt pavement under vehicle loading. *Appl. Sci.* **2020**, *10*, 1416. [CrossRef]
72. Dong, Q.; Li, Y.; Shi, X.; Li, Z. Calculation and Analysis of Dynamic Water Pressure on Road Surfaces. *J. Chang. Univ. (Nat. Sci. Ed.)* **2013**, *33*, 17–22.
73. Zhang, Y.; Gu, X.; Xing, S.; Wang, X.; Cui, B. Study on Dynamic Water Pressure of Asphalt Pavement Structure Based on COMSOL Fluid-Solid Coupling. *Munic. Eng. Technol.* **2020**, *38*, 48–52+64. [CrossRef]
74. Yi, J.; Feng, D.; Yang, S.H.; Yu, F. A Preliminary Analysis on Determination of Optimum Crack Sealing Time for Asphalt Pavement (No. 13-1336). In Proceedings of the Transportation Research Board, Washington, DC, USA, 13–17 January 2013. [CrossRef]
75. Mousa, M.; Elseifi, M.A.; Bashar, M.; Zhang, Z.; Gaspard, K. Field evaluation and cost effectiveness of crack sealing in flexible and composite pavements. *Transp. Res. Rec.* **2018**, *2672*, 51–61. [CrossRef]
76. Mousa, M.R.; Elseifi, M.A.; Bashar, M.Z.; Zhang, Z.; Gaspard, K.; Free, K. Cost effectiveness and optimal timing of crack sealing in asphalt concrete overlays. *J. Transp. Eng. Part B Pavements* **2019**, *145*, 04019029. [CrossRef]
77. Yue, G.; Du, Y.; Liu, C.; Guo, S.; Li, Y.; Gao, Q. Road subsurface distress recognition method using multiattribute feature fusion with ground penetrating radar. *Int. J. Pavement Eng.* **2023**, *24*, 2037591. [CrossRef]
78. Zhao, W.; Yang, Q. Evaluation of Fatigue Performance of Old Cement Concrete Pavement Based Three-Dimensional Ground On Penetrating Radar and Falling Weight Deflectometer. *J. Tongji Univ. (Nat. Sci.)* **2025**, *53*, 732–740. [CrossRef]
79. Wang, D.W.; Lyu, H.T.; Tang, F.J.; Ye, C.S.; Zhang, F.; Wang, S.Q.; Ni, Y.W.; Leng, Z.; Lu, G.Y.; Liu, P.F. Review on Detection Analysis and Digital Technology for Road Hidden Diseases Using 3D Ground Penetrating Radar. *Zhongguo Gonglu Xuebao/China J. Highw. Transp.* **2023**, *36*, 1–19.
80. Liu, W.; Luo, R.; Xiao, M.; Chen, Y. Intelligent detection of hidden distresses in asphalt pavement based on GPR and deep learning algorithm. *Constr. Build. Mater.* **2024**, *416*, 135089. [CrossRef]
81. Liu, C.; Du, Y.; Yue, G.; Li, Y.; Wu, D.; Li, F. Advances in automatic identification of road subsurface distress using ground penetrating radar: State of the art and future trends. *Autom. Constr.* **2024**, *158*, 105185. [CrossRef]
82. Dou, Q.; Wei, L.; Magee, D.R.; Cohn, A.G. Real-time hyperbola recognition and fitting in GPR data. *IEEE Trans. Geosci. Remote Sens.* **2016**, *55*, 51–62. [CrossRef]
83. Liu, C.; Yao, Y.; Li, J.; Qian, J.; Liu, L. Research on lightweight GPR road surface disease image recognition and data expansion algorithm based on YOLO and GAN. *Case Stud. Constr. Mater.* **2024**, *20*, e02779. [CrossRef]
84. Harkat, H.; Bennani, H.D. Ground penetrating radar imaging for buried cavities in a dispersive medium: Profile reconstruction using a modified hough transform approach and a time-frequency analysis. *Int. J. Commun. Antenna Propag. (IRECAP)* **2015**, *5*, 78–92. [CrossRef]

85. Solla, M.; Lagüela, S.; González-Jorge, H.; Arias, P. Approach to identify cracking in asphalt pavement using GPR and infrared thermographic methods: Preliminary findings. *NDT E Int.* **2014**, *62*, 55–65. [CrossRef]
86. Guo, S.; Xu, Z.; Li, X.; Zhu, P. Detection and characterization of cracks in highway pavement with the amplitude variation of GPR Diffracted waves: Insights from forward modeling and field data. *Remote Sens.* **2022**, *14*, 976. [CrossRef]
87. Yang, J.; Yang, S.; Yao, Y.; Gao, J.; Wang, S. Three-dimensional orthorectified simulation and ground penetrating radar detection of interlayer bonding condition in asphalt pavements. *Meas. Sci. Technol.* **2024**, *35*, 095017. [CrossRef]
88. Marecos, V.; Solla, M.; Fontul, S.; Antunes, V. Assessing the pavement subgrade by combining different non-destructive methods. *Constr. Build. Mater.* **2017**, *135*, 76–85. [CrossRef]
89. Wang, S.; Leng, Z.; Sui, X. Detectability of concealed cracks in the asphalt pavement layer using air-coupled ground-penetrating radar. *Measurement* **2023**, *208*, 112427. [CrossRef]
90. Su, J.; Shi, J.; Wang, W. Experimental Study of Infrared Thermal lmagers about Influence of Distance for Temperature Measurement Accuracy and Method of lmproving Accuracy. *Infrared Technol.* **2013**, *35*, 587–590.
91. Chen, W.; Wei, K.; Wei, J.; Han, W.; Zhang, X.; Hu, G.; Wei, S.; Niu, L.; Chen, K.; Fu, Z.; et al. Research on the road performance of asphalt mixtures based on infrared thermography. *Materials* **2022**, *15*, 4309. [CrossRef]
92. Vyas, V.; Patil, V.J.; Singh, A.P.; Srivastava, A. Application of infrared thermography for debonding detection in asphalt pavements. *J. Civ. Struct. Health Monit.* **2019**, *9*, 325–337. [CrossRef]
93. Singla, R.; Sharma, S.; Siddique, R. Monitoring of chemical-assisted healing of fine cracks in concrete using ultrasonics and infrared thermographic techniques. *J. Build. Eng.* **2025**, *104*, 112279. [CrossRef]
94. Liu, F.; Liu, J.; Wang, L. Deep learning and infrared thermography for asphalt pavement crack severity classification. *Autom. Constr.* **2022**, *140*, 104383. [CrossRef]
95. Du, Y.; Zhang, X.; Li, F.; Sun, L. Detection of crack growth in asphalt pavement through use of infrared imaging. *Transp. Res. Rec.* **2017**, *2645*, 24–31. [CrossRef]
96. Golrokh, A.J.; Gu, X.; Lu, Y. Real-time thermal imaging-based system for asphalt pavement surface distress inspection and 3D crack profiling. *J. Perform. Constr. Facil.* **2021**, *35*, 04020143. [CrossRef]
97. Liu, F.; Liu, J.; Wang, L.; Al-Qadi, I.L. Multiple-type distress detection in asphalt concrete pavement using infrared thermography and deep learning. *Autom. Constr.* **2024**, *161*, 105355. [CrossRef]
98. Yang, X.; Huang, R.; Meng, Y.; Liang, J.; Rong, H.; Liu, Y.; Tan, S.; He, X.; Feng, Y. Overview of the application of Ground-Penetrating Radar, Laser, infrared thermal Imaging, and ultrasonic in nondestructive testing of road surface. *Measurement* **2024**, *224*, 113927. [CrossRef]
99. Tang, N.; Guo, S.; Yang, Y.; Sun, W. Ultrasonic waves generated by smart aggregates for concealed crack detection in asphalt mixture. *Constr. Build. Mater.* **2024**, *438*, 137183. [CrossRef]
100. Pan, W.H.; Sun, X.D.; Wu, L.M.; Yang, K.K.; Tang, N. Damage detection of asphalt concrete using piezo-ultrasonic wave technology. *Materials* **2019**, *12*, 443. [CrossRef]
101. Franesqui, M.A.; Yepes, J.; García-González, C. Ultrasound data for laboratory calibration of an analytical model to calculate crack depth on asphalt pavements. *Data Brief* **2017**, *13*, 723–730. [CrossRef] [PubMed]
102. Franesqui, M.A.; Gallego, J. Inspection and depth sizing of surface-initiated cracking for preventive maintenance of asphalt pavements. *Int. J. Pavement Eng.* **2023**, *24*, 2083617. [CrossRef]
103. Zhang, W.; Akber, M.A.; Hou, S.; Bian, J.; Zhang, D.; Le, Q. Detection of dynamic modulus and crack properties of asphalt pavement using a non-destructive ultrasonic wave method. *Appl. Sci.* **2019**, *9*, 2946. [CrossRef]
104. Li, S. Study on Nondestructive Testing Technology Based on Ground Penetrating Radar and Ultrasonic Testing in Pavements. Master's Thesis, Southeast University, Nanjing, China, 2021.
105. Liu, Z.; Gu, X.; Wu, C.; Ren, H.; Zhou, Z.; Tang, S. Studies on the validity of strain sensors for pavement monitoring: A case study for a fiber Bragg grating sensor and resistive sensor. *Constr. Build. Mater.* **2022**, *321*, 126085. [CrossRef]
106. Liu, Z.; Zhu, G.; Liu, L.; Li, W.; Fu, S. Integrated Design Method for Built-in Sensing Devices and Asphalt Pavement Considering Cooperative Deformation Enhancement. *J. Chang. Univ. Sci. Technol. (Nat. Sci. Ed.)* **2023**, *19*, 131–142.
107. Chen, Z.; Wang, Z.; Li, X.; Lin, Y.; Luo, N.; Long, M.; Zhao, N.; Xu, J.-B. Flexible piezoelectric-induced pressure sensors for static measurements based on nanowires/graphene heterostructures. *ACS Nano* **2017**, *11*, 4507–4513. [CrossRef]
108. Shi, J.; Wang, L.; Dai, Z.; Zhao, L.; Du, M.; Li, H.; Fang, Y. Multiscale hierarchical design of a flexible piezoresistive pressure sensor with high sensitivity and wide linearity range. *Small* **2018**, *14*, 1800819. [CrossRef]
109. Weng, S.; Zhang, Z.; Gao, K.; Zhu, H. Research progress of flexible piezoresistive strain sensing technology in structural health monitoring. *J. Build. Struct.* **2024**, *45*, 242–261. [CrossRef]
110. Yi, H.; Wang, S.; Mei, S.; Li, Z. Conductive polymer composites for resistive flexible strain sensors. *Polymer* **2024**, *307*, 127286. [CrossRef]

111. Huang, P.; Wang, T.; Zhou, Y.; Fan, Y.; Wu, Y.; Wang, H.; Yang, J.; Huang, W. Piezoresistive response of MWCNTs/Epoxy mixtures with load-sensing capability. *Constr. Build. Mater.* **2024**, *438*, 137203. [CrossRef]
112. Xin, X.; Qiu, Z.; Luan, X.; Ding, X.; Liang, M.; Yao, Z.; Li, Y. Novel conductive polymer composites for asphalt pavement structure in situ strain monitoring: Influence of CB/CNT and GNP/CNT nano/micro hybrid fillers on strain sensing behavior. *IEEE Sens. J.* **2022**, *22*, 3945–3956. [CrossRef]
113. Gulisano, F.; Buasiri, T.; Apaza, F.R.A.; Cwirzen, A.; Gallego, J. Piezoresistive behavior of electric arc furnace slag and graphene nanoplatelets asphalt mixtures for self-sensing pavements. *Autom. Constr.* **2022**, *142*, 104534. [CrossRef]
114. Rizvi, H.R.; Khattak, M.J.; Madani, M.; Khattab, A. Piezoresistive response of conductive Hot Mix Asphalt mixtures modified with carbon nanofibers. *Constr. Build. Mater.* **2016**, *106*, 618–631. [CrossRef]
115. Liu, X.M.; Wu, S.P. Study on the piezoresistivity character of electrically conductive asphalt concrete. *Adv. Mater. Res.* **2011**, *233*, 1756–1761. [CrossRef]
116. Ruschau, G.R.; Yoshikawa, S.; Newnham, R.E. Resistivities of conductive composites. *J. Appl. Phys.* **1992**, *72*, 953–959. [CrossRef]
117. Garcia, J.R.; O'Suilleabhain, D.; Kaur, H.; Coleman, J.N. A simple model relating gauge factor to filler loading in nanocomposite strain sensors. *ACS Appl. Nano Mater.* **2021**, *4*, 2876–2886. [CrossRef]
118. Xin, X.; Liang, M.; Yao, Z.; Su, L.; Zhang, J.; Li, P.; Sun, C.; Jiang, H. Self-sensing behavior and mechanical properties of carbon nanotubes/epoxy resin composite for asphalt pavement strain monitoring. *Constr. Build. Mater.* **2020**, *257*, 119404. [CrossRef]
119. Xin, X.; Luan, X.; Su, L.; Ma, C.; Liang, M.; Ding, X.; Yao, Z. The innovative self-sensing strain sensor for asphalt pavement structure: Substitutability and synergy effects of graphene platelets with carbon nanotubes in epoxy composites. *Front. Mater.* **2022**, *9*, 824364. [CrossRef]
120. Wang, Z.; Feng, Z.G.; Cui, Q.; Guang, G.; Li, X. Evaluation of piezoresistive response and mechanical performance of self-sensing asphalt concrete mixed with different lengths of carbon fiber. *Constr. Build. Mater.* **2025**, *462*, 139942. [CrossRef]
121. Li, D. Cement-Based Piezoresistive Sensors and Fatigue Properties of Embedded Components. Mater's Thesis, Tsinghua University, Beijing, China, 2021. [CrossRef]
122. Xu, X. Mechanical properties and sensing properties of embedded ngraphene cement-based sensor. Mater's Thesis, Chang'an University, Xian, China, 2024. [CrossRef]
123. Gao, L.; Ding, S.; She, J.; Zhang, J.; He, R. Research Status of Piezoelectric Technology Application in Intelligent Road. *Sci. Technol. Eng.* **2023**, *23*, 11486–11495. [CrossRef]
124. Zhao, H.; Qin, L.; Ling, J. Synergistic performance of piezoelectric transducers and asphalt pavement. *Int. J. Pavement Res. Technol.* **2018**, *11*, 381–387. [CrossRef]
125. Cain, M.G.; Stewart, M. Standards for piezoelectric and ferroelectric ceramics. In *Characterisation of Ferroelectric Bulk Materials and Thin Films*; Springer: Dordrecht, The Netherlands, 2014; pp. 267–275.
126. Jiang, W.; Li, P.; Sha, A.; Li, Y.; Yuan, D.; Xiao, J.; Xing, C. Research on pavement traffic load state perception based on the piezoelectric effect. *IEEE Trans. Intell. Transp. Syst.* **2023**, *24*, 8264–8278. [CrossRef]
127. Zhu, X.; Zhou, X.; Ye, F.; Wu, H.; Du, Z. Development and evaluation of cement/emulsified-asphalt based piezoelectric sensors for road weigh-in-motion system. *Smart Mater. Struct.* **2021**, *30*, 125013. [CrossRef]
128. He, H.; Huang, J.; Zhao, Q.; Tan, Q.; Zang, X. Self-powered asphalt-based sensors for smart roads. *Nano Energy* **2025**, *134*, 110525. [CrossRef]
129. Sebaaly, P.E.; Tabatabaee, N.; Kulakowski, B. Evaluation of the hall effect sensor for pavement instrumentation. *J. Test. Eval.* **1995**, *23*, 189–195. [CrossRef]
130. Wang, J.; Han, Y.; Cao, Z.; Xu, X.; Zhang, J.; Xiao, F. Applications of optical fiber sensor in pavement Engineering: A review. *Constr. Build. Mater.* **2023**, *400*, 132713. [CrossRef]
131. Kashaganova, G.; Kozbakova, A.; Kartbayev, T.; Balbayev, G.; Togzhanova, K.; Alimseitova, Z.; Orazaliyeva, S. Research of a fiber sensor based on fiber Bragg grating for road surface monitoring. *Electronics* **2023**, *12*, 2491. [CrossRef]
132. Sundaram, B.A.; Ravisankar, K.; Senthil, R.; Parivallal, S. Wireless sensors for structural health monitoring and damage detection techniques. *Curr. Sci.* **2013**, *104*, 1496–1505.
133. Xiao, J.; Zou, X.; Xu, W. ePave: A self-powered wireless sensor for smart and autonomous pavement. *Sensors* **2017**, *17*, 2207. [CrossRef] [PubMed]
134. Alavi, A.H.; Hasni, H.; Lajnef, N.; Chatti, K. Continuous health monitoring of pavement systems using smart sensing technology. *Constr. Build. Mater.* **2016**, *114*, 719–736. [CrossRef]
135. Hasni, H.; Alavi, A.H.; Jiao, P.; Lajnef, N.; Chatti, K.; Aono, K.; Chakrabartty, S. A new approach for damage detection in asphalt concrete pavements using battery-free wireless sensors with non-constant injection rates. *Measurement* **2017**, *110*, 217–229. [CrossRef]
136. Ji, X.; Hou, Y.; Chen, Y.; Zhen, Y. Fabrication and performance of a self-powered damage-detection aggregate for asphalt pavement. *Mater. Des.* **2019**, *179*, 107890. [CrossRef]

137. Fu, B.; Li, P.; Zhang, Y.; Zheng, S.; Wang, Y. Research on damage recognition of concrete beams based on embedded piezoelectric sensors. *Case Stud. Constr. Mater.* **2025**, *22*, e04769. [CrossRef]
138. Xiong, H.; Wang, L. Piezoelectric energy harvester for public roadway: On-site installation and evaluation. *Appl. Energy* **2016**, *174*, 101–107.

Disclaimer/Publisher's Note: The statements, opinions and data contained in all publications are solely those of the individual author(s) and contributor(s) and not of MDPI and/or the editor(s). MDPI and/or the editor(s) disclaim responsibility for any injury to people or property resulting from any ideas, methods, instructions or products referred to in the content.